STATISTICAL THERMODYNAMICS OF LONG-RANGE QUANTUM SPIN SYSTEMS

By

G. J. F. OLIVIER

Thesis presented in partial fulfilment of the requirements for the degree of
MASTER OF SCIENCE at the University of Stellenbosch.

Supervisor : Professor Michael Kastner

March 2012

DECLARATION

By submitting this thesis electronically, I declare that the entirety of the work contained therein is my own, original work, that I am the sole author thereof (save to the extent explicitly otherwise stated), that reproduction and publication thereof by Stellenbosch University will not infringe any third party rights and that I have not previously in its entirety or in part submitted it for abtaining any qualification.

Abstract

In this thesis we discuss some of the anomalies present in systems with long-range interactions, for instance negative specific heat and negative magnetic susceptibility, and show how they can be related to the convexity properties of the thermodynamic potentials and non-equivalence of ensembles. We also discuss the possibility of engineering long-range quantum spin systems with cold atoms in optical lattices to experimentally verify the existence of non-equivalence of ensembles. We then formulate an expression for the density of states when the energy and magnetisation correspond to a pair of non-commuting operators. Finally we analytically compute the entropy $\mathrm{s}(\epsilon, \underline{m})$ as a function of energy, ϵ, and magnetisation, $\underline{m}$, for the anisotropic Heisenberg model with Curie-Weiss type interactions. The results show that the entropy is non-concave in terms of magnetisation under certain circumstances which in turn indicates that the microcanonical and canonical ensembles are not equivalent and that the magnetic susceptibility is negative. After making an appropriate change of variables we show that a second-order phase transition can be present at negative temperatures in the microcanonical ensemble which cannot be represented in the canonical ensemble.

Opsomming

In hierdie tesis bespreek ons van die onverwagte eienskappe wat sisteme met lang afstand wisselwerkings kan openbaar, byvoorbeeld negatiewe spesifieke warmte en negatiewe magnetiese suseptibiliteit. Ons dui ook die ooreenkoms tussen hierdie gedrag en die konveksiteit van die termodinamiese potensiale en nie-ekwivalente ensembles aan. Hierna bespreek ons die moontlikheid om lang afstand kwantum spin sisteme te realiseer met koue atome in 'n optiese rooster. Daarna wys ons hoe dit moontlik is om 'n uitdrukking vir die digtheid van toestande te formuleer vir sisteme waar die energie en magnetisasie ooreenstem met operatore wat nie met mekaar kommuteer nie. Uiteindelik bepaal ons die entropie, $s(\epsilon, \underline{m})$, in terme van die energie, ϵ, en magnetisasie, m, vir die anisotropiese Heisenberg model met Curie-Weiss tipe interaksies. Die resultate wys dat die entropie onder sekere omstandighede nie konkaaf in terme van magnetisasie is nie. Dit, op sy beurt, dui aan dat die mikrokanoniese en kanoniese ensembles nie ekwivalent is nie en dat die magnetiese suseptibiliteit negatief kan wees. Nadat ons 'n toepaslike transformasie van veranderlikes maak, wys ons dat 'n tweede orde fase-oorgang by negatiewe temperature kan plaasvind in die mikrokanoniese ensemble wat nie verteenwoordig kan word in die kanoniese ensemble nie.

Acknowledgments

I would like to sincerely thank my supervisor, Professor Michael Kastner, for the guidance he has given me during the past two years. Not only for pointing me in the right direction when I was at a dead end with my project, but also his patience, dedication and positive attitude served as a great source of inspiration.

Thanks to the National Institute for Theoretical Physics, for providing financial support for my studies during my M.Sc. and for awarding travel grants to attend conferences and summer schools. I am thankful for the privilege of having received it.

I would also like to thank my fellow students at the department for the making the tough times bearable, especially Marisa Geyer for her help, support and friendship.

Lastly, I would like to thank my family for their encouragement and continued support.

LIST OF FIGURES

CONTENTS

CHAPTER 1
Introduction

Long-range interacting systems are widely present in nature, with self gravitating systems [1], non-neutral plasmas [2], free electron lasers [3] and many more [4] [7] [10]. For this reason alone it is essential that we include these systems in the formulation of equilibrium thermodynamics. The majority of research within statistical physics on systems with long-range interactions consider situations where gravity is the dominant interaction between constituent particles. The reason for this is simply because in systems where interactions are electromagnetic of kind, screening between positive and negative charges takes place so that interactions of finite range approximate these systems well. In gravitating systems this is of course not the case since masses are non-negative.

In general, equivalence of ensembles holds for all systems with short-range interactions. The proof of this consists of partitioning a system into smaller subsystems and then in the thermodynamic limit neglecting the boundary interactions of the various subsystems. In systems with long-range interactions this is not always the case since the boundary effects cannot be neglected because of the long-range nature of the interactions. This gives rise to various anomalies unique to systems with long-range interactions, for example negative specific heat, negative magnetic susceptibility and non-equivalence of ensembles.

The reason why we are interested in studying different statistical ensembles is because they correspond to different physical situations, realised for example in solid state physics and cold atomic physics. It would therefore be interesting to study the same long-range model in these different physical situations and compare the results, since the different ensembles may be non-equivalent for systems with long-range interactions. In order to do this we need to consider a model that can be realised in different physical situations that correspond to different statistical ensembles.

To achieve this goal we will consider a quantum spin system with long-range interactions. This system should be realisable with cold atoms in optical lattices, where the appropriate statistical ensemble is the microcanonical one. During this thesis we will calculate the entropy of this system by taking into account that the energy and magnetisation correspond to a pair of non-commuting operators. Historically, the model we will consider has been studied in the canonical setting, so that the canonical results are known [5]. This will enable us to compare the results obtained in the different statistical ensembles. Although the model we will consider provides the simplest example of a long-range quantum system that can be realised in the

microcanonical setting, the idea is to illustrate the differences between the two statistical ensembles for these types of systems in general.

One of the ideas of this thesis is to add to the number of exact calculations of long-range interacting quantum systems in the microcanonical ensemble. These calculations do not appear frequently in the literature. The paper by Pflug [6] on gravitating fermions is a notable example where negative specific heat is found for a certain energy range. For classical long-range systems, there are numerous microcanonical results reported, for a review on this see [4] [7] [10]. The reasons for the lack of results reported for long-range quantum systems in the microcanonical setting are twofold. Firstly, calculating the microcanonical density of states is generally more difficult than computing the canonical partition function. Secondly, it is not yet well established how to define a microcanonical density of states in terms of two variables that correspond to non-commuting operators, which can be the case for quantum systems.

Throughout the first four chapters we will justify our interest in studying systems with long-range interactions by discussing some of the unexpected behaviour that might occur in these systems. We also show the relationship between these anomalies and the convexity properties of the thermodynamic potentials. During chapter 5 we will propose a possible experimental concept where long-range quantum spin systems can be engineered with cold atoms in optical lattices and studied to add to the limited knowledge of these systems. In chapter 6 we introduce the model we are considering, which is an extension of the model studied in [26], and proceed to the exact solution of the system in chapter 7 and 8. The details of the formulation and calculation in chapter 7 and 8 are quite technical in nature. The results will be discussed in chapter 9 , which show that the canonical and microcanonical ensembles are not equivalent for certain parameters of the model and that the magnetic susceptibility of the system can be negative. Additionally we show that phase transitions may occur at negative temperatures in the microcanonical setting, while in the canonical setting the temperature is usually assumed to be strictly positive.

These results imply that quantum spin systems can exhibit behaviour in the cold atomic setting that can not be illustrated in a canonical condensed matter setting. Therefore using results obtained in the canonical ensemble to try and predict the behaviour of long-range systems engineered with cold atoms in optical lattices will be insufficient. We conclude the thesis with a discussion of the main results and provide an outlook for possible research that could extend on this thesis.

CHAPTER 2
Long-range interacting systems

Systems with long-range interactions display certain characteristics that seem unexpected. Throughout this chapter I will mention and give some examples of these anomalies and then in chapter 3 and 4 explain the physical reason why these anomalies occur. Before we get started we should define how we distinguish between short- and long-range interactions properly. The widely accepted [10] [7] definition is that for a interaction potential between two particles that decay proportionally to $1/r^{d+\alpha}$ with distance r, the system can be classified as **long-range** if $-d \leq \alpha \leq 0$ and **short-range** if $\alpha > 0$, where d is the dimension of the system. This definition might seem arbitrary at this stage but in section 3.2 the reason for this distinction will become clear.

2.1 Specific heat and magnetic susceptibility

The existence of negative specific heat can be declared as the most unintuitive characteristic of long-range interacting systems in my opinion. Indeed pumping heat into a system in order to lower its temperature does not seem to be physically realisable, but for long-range interactions it is. This concept has long been known in astrophysics [11]. The process relates for instance to stars who have used up their nuclear fuel and radiate energy to contract and heat up [12]. The relation between negative specific heat and statistical mechanics was proposed much later, when Thirring showed in [12] that in the region where the microcanonical specific heat of self-gravitating gas spheres [13] is negative, the statistical ensembles are non-equivalent. Specific heat may become negative close to a phase transition. For a gravitational system this corresponds to the transition between a 'clustered' and a 'gas' phase. Although the presence of negative magnetic susceptibility may not seem as spectacular as negative specific heat it can be regarded as the magnetisation equivalent to it, which is a distinct property of systems with long-range interactions. As with specific heat, magnetic susceptibility may become negative close to a phase transition. In magnetic systems, this phase transition is between a ferromagnetic and paramagnetic phase. Both these quantities can only be negative in the microcanonical ensemble, as will be shown in chapter 4. This fact indicates that the microcanonical and canonical ensembles can in some circumstances be non-equivalent.

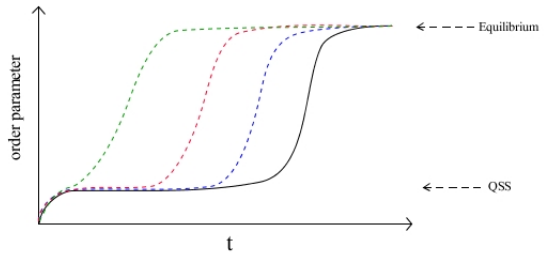

Figure 2.1: An example of a system trapped in a quasi-stationary state for some order parameter. Here the QSS pointer indicates the quasi-stationary state and the equilibrium state is indicated by the equilibrium pointer. In the figure the size of the system is different for every line, with the green dotted line being the smallest and the black solid line being the largest. Note that the equilibration time diverges with system size and the system is trapped in the quasi-stationary state for a large fraction of the equilibration time when the system is large.

2.2 Quasi-stationary states

Recent results for systems with long-range interactions indicate that equilibration time might diverge with system size. Not only does the equilibration time diverge, but the system appears to be trapped in quasi-stationary states. These quasi-stationary states can easily be misinterpreted as equilibrium states when doing experiments. In figure 2.1 a typical example of a quasi-stationary state is shown, where the system is trapped in a state before it equilibrates to the actual equilibrium state. Examples of this phenomenon are the formation of binary stars and globular clusters in astrophysical systems where the equilibration time toward gravothermal collapse is much larger than the age of the universe [14]. It should be noted that equilibration times for short-range systems might also be large. A recent experiment [15] illustrated that, even for a system with short-range interactions, no equilibration was observed on the time scale of the experiment. Although the equilibration time here is large, it converges to a finite value in the large system limit. This is an important property we need to acknowledge when discussing possible experimental realisations in chapter 5. We are crossing into the domain of out-of-equilibrium dynamics of long-range systems here, which we will not discuss in any detail. For the remainder of the thesis we will discuss Boltzmann-Gibbs equilibrium statistical mechanics.

2.3 Non-equivalence of ensembles

The previously mentioned anomalies are striking physical properties of long-range systems. The presence of these irregularities are related to non-equivalent ensembles. This relation

will be discussed in chapter 4. In short-range interacting systems or long-range tempered interactions, in the thermodynamic limit, the different statistical ensembles are equivalent. This is proved in [16]. The significance of this is that no matter in which ensemble the system is prepared, only one of the thermodynamic potentials has to be calculated (even if it is not in the appropriate setting) since the other can be recovered by means of the Legendre-Fenchel transform, discussed in section 4.1. This is a very convenient property, since in most cases the microcanonical entropy is harder to compute than the canonical free energy. For systems with long-range interactions this statement and proof do not hold. This property was at first regarded by skeptics as a flaw in the formulation of equilibrium statistical mechanics, but since then it has been shown that the existence of non-equivalent ensembles is a physical property of the setting that the system is prepared in. This statement can be clarified by the fact that non-equivalent ensembles have non-equivalent equilibrium macrostates [22]. Therefore if for instance we have a long-range system with fixed energy and particle number, it could equilibrate to an equilibrium macrostate that does not have a corresponding macrostate for a system with fixed particle number at any temperature.

CHAPTER 3
Extensivity and additivity

In thermodynamics, additivity is crucial for a number of fundamental proofs (for instance proving equivalence of ensembles for short-range systems in the thermodynamic limit). In this chapter we will show, by an example, that systems with long-range interactions are not necessarily additive even if they are extensive and that systems with short-range interactions are usually additive when they are extensive. When making claims about extensivity and additivity we must be careful since one does not imply the other. Before we go any further we should define what is meant by extensivity and additivity.

A physical quantity is said to be **extensive** if it is proportional the size of the system [8]. In thermodynamics, entropy, energy and free energy are assumed to be extensive. Pressure and temperature, however, are not extensive (intensive) since these parameters are not dependent on system size.

Additivity is a property of a system that states that when you divide a system into macroscopic parts, the total energy is equal to sum of the energies of the macroscopic parts [8]. Therefore the boundary effects of the macroscopic subsystems are negligible. The energy for an arbitrary system is given by $U = U_1 + U_2 + U_{int}$, where U_1 and U_2 are the energies of the two macroscopic parts and U_{int} is the interaction energy between the two parts (boundary effects). If the system is additive we know that U_1,$U_2 \gg U_{int}$ so that $U \approx U_1 + U_2$ in the thermodynamic limit.

From the definitions given above it is clear that the two properties are related, but not equivalent. This is a common misperception in the statistical physics community. It can be said that additivity usually implies extensivity, but a stronger statement cannot be made since extensivity may be dependent on the scaling factor that is implemented. Systems that are non-extensive, but that can be made extensive (or vice-versa) by introducing a scaling factor can be referred to as pseudo-extensive. A well known example of this for mean-field systems is the so-called Kac prescription, which will be discussed in chapter 3.2.

Long-range systems are not additive, even if they are extensive (or pseudo-extensive). This is because if you divide a long-range system into macroscopic parts and consider the thermodynamic limit, the interactions between neighbouring subsystems cannot be neglected. This comes from the long-range nature of the interactions between the particles of the subsystems. It differs from short-range interactions where the boundary interaction become negligible in the thermodynamic limit.

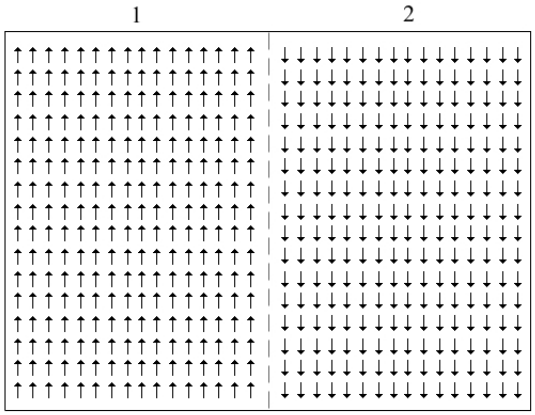

Figure 3.1: $2N$ **spin-1 particle lattice system. The spins in system 1 (left hand side) are all pointing upwards and the spins in system 2 (right hand side) are all pointing downward.**

3.1 Examples

To illustrate these concepts, consider the Ising model on a lattice consisting of $2N$ particles. This example and explanation is similar to the discussion in [7]. To make it even more simple consider a configuration where the N particles on the left are all pointing up and the N particles on the right are all pointing down. Also let us consider the system in a zero external magnetic field with all the lattice sites assumed to be the same. This configuration is illustrated in figure 3.1. The Hamiltonian of the system is given by

$$H = -\frac{J}{C_N}\sum_{i=1}^{2N}\sum_{j=1}^{2N}\frac{S_i S_{i+j}}{r_{ij}^{\alpha}} \tag{3.1}$$

Here $i, j \in \{1, \cdots, 2N\}$ and $i \neq j$ and $S = \pm 1$ depending if the spins are pointing up (+) or down (-). The denominator in the sum, r_{ij}, is the distance between particles at sites i and j, with α the rate at which the interaction strength decays. If $0 \leq \alpha \leq 1$ we have long-range interactions and if $\alpha > 1$ we have short range interactions according to the definition above. The lattice sites are numbered from 1 to $2N$ and are periodic so that $i + 2N = i$. The factor $1/C_N$ is the normalization factor and is responsible for making the model extensive. The choice of this normalization factor will depend on the interaction strength and the exact α dependence of this factor is shown in section 3.2. We will consider two different scenarios, one with mean-field type interactions and one with nearest-neighbour type interactions (so that the sum is only over nearest neighbours). These are two extreme cases of long- and short-range interactions respectively. We split the system into two N-particle systems labeled 1 and 2 as in figure 3.1.

3.1.1 Mean-field interactions

For the mean-field type interactions ($\alpha = 0$), each particle is interacting with every other of the $2N - 1$ particles with equal strength so the Hamiltonian can be written as

$$H = -\frac{J}{2N}\sum_{i=1}^{2N}\sum_{j=1}^{2N} S_i S_{i+j} = -\frac{J}{2N}\left(\sum_{i=1}^{2N} S_i\right)^2. \tag{3.2}$$

where $C_N = \frac{1}{2N}$ has already been chosen. The total energy for the configuration in figure 3.1 is therefore given by

$$U(1+2) = 0, \tag{3.3}$$

since there are an equal number of spins pointing up and down. But if we consider systems one and two separately we find that system one has energy $U(1) = -\frac{JN}{2}$ and system two also has energy $U(2) = -\frac{JN}{2}$ so that the sum of the energies of the system are

$$U(1) + U(2) = -JN. \tag{3.4}$$

Notice that this expression is valid in the thermodynamic limit so we can clearly confirm the system is not additive,

$$U(1+2) \neq U(1) + U(2), \tag{3.5}$$

but extensive. Of course this was expected since the boundary effects here are not negligible

3.1.2 Nearest-neighbour interactions

If we now consider the short-range case where each particle only interacts with its nearest-neighbour ($r = 1$), we can write the Hamiltonian as

$$H = -J\sum_{\langle i,j\rangle} S_i S_j. \tag{3.6}$$

with $C_N = 1$. The triangular brackets in the sum denote the sum over all pairs of nearest neighbours. In this case our notation is unconventional considering the original Hamiltonian and deserves some explanation. Because we only consider nearest-neighbour interactions on the two-dimensional square lattice sketched in figure 3.1 we exclude the interaction distance term $\frac{1}{r_{ij}^{\alpha}}$ since the interaction distance is one for nearest neighbours. It is straightforward to verify that the energy of the total system is given by

$$U(1+2) = -8JN + 10J\sqrt{N}, \tag{3.7}$$

while the energies of the subsystems are given by $U(1) = U(2) = -4JN + 4J\sqrt{N}$, so that

$$U(1) + U(2) = -8JN + 8J\sqrt{N}. \tag{3.8}$$

If we rewrite these expressions as

$$U(1+2) = -8JN\left(1 - \frac{5}{4\sqrt{N}}\right), \tag{3.9}$$

$$U(1) + U(2) = -8JN\left(1 - \frac{1}{\sqrt{N}}\right), \tag{3.10}$$

it is now clear that in the limit, $N \to \infty$, $U(1+2) \approx U(1) + U(2) \approx -8JN$. Hence the system is additive. Notice here that the $1/N$ factor is not present in the Hamiltonian since the energy is extensive and scales as N without this factor. In the following section, we will discuss the choice of the scaling factor and why it is necessary for the energy to scale as N.

Although the interactions chosen in this example were two extreme cases of long- and short-range interactions, it can be shown in general that systems with short-range interactions are additive and systems with long-range interactions are not necessarily since the interaction energy between subsystems might scale with the system size. The unique properties of systems with long-range interactions, that were mentioned in chapter 2, are due to this non-additivity property.

3.2 Scaling factor and the Kac prescription

In the preceding example there was a scaling factor of $1/N$ present in the Hamiltonian for the long-range case which ensured that the energy was extensive and scaled as N. This $1/N$ factor was first introduced by Baker [17] for the mean-field Ising model.

To explain the choice of the scaling factor, let us first explain what the aim is when introducing such a factor. Consider a repulsive potential that is exponentially decreasing with interaction distance,

$$\phi(x) = -\alpha e^{-\gamma x}. \tag{3.11}$$

If we take the limit $\gamma \to 0$ (mean field type interactions) the energy of the system is not extensive and the usual thermodynamic potentials diverge in the thermodynamic limit. In [18], Kac et al. show that if you however impose $\alpha = \alpha_0\gamma$ and consider the limit again, the energy is extensive and the system exhibits a phase transition. This is commonly referred to as the Kac prescription or Kac's trick.

The trick mentioned above is analogous, although the limit is not the same, to the $1/N$

factor present in the Hamiltonian for the long-range case. The reason why the system can in principle exhibit a phase transition in this case has to do with the scaling of the energy. From the formulation of equilibrium statistical mechanics, the density of states grows exponentially with system size, which in turn implies that the entropy (which is the logarithm of the density of states) scales linearly with system size and must therefore be extensive. This statement is true regardless of the nature of the interactions.

Now consider the expression for the free-energy $F = U - TS$. The temperature is intensive, it does not scale with system size. In order to observe a phase transition we need the energy, U, and entropy, S, to compete. Since the entropy is assumed to be extensive we need to scale the energy so that it also scales linearly with system size. This is why in [18], Kac's trick caused the system to exhibit a phase transition and also why we need the $1/N$ factor for the mean field case of the Ising model we considered.

Here we might wonder why there is no scaling factor for the nearest-neighbour case. It is clear that the energy scales linearly with N without this prefactor but what about the cases in between? Here the definition of long-range interactions becomes important. In order to find the exact scaling properties of the system, consider the N particle Hamiltonian for the Ising model on a one-dimensional periodic lattice,

$$H = -\frac{J}{C_N}\left(\sum_{i=1}^{N}\sum_{j=1}^{N-1}\frac{S_i S_{i+j}}{j^\alpha}\right), \tag{3.12}$$

here the distance between interacting particles is simply j since the lattice is one-dimensional. Now since $S_i S_j = \pm 1$,

$$-\frac{J}{C_N}\sum_{i=1}^{N}\sum_{j=1}^{N-1}\frac{1}{j^\alpha} \leq H \leq \frac{J}{C_N}\sum_{i=1}^{N}\sum_{j=1}^{N-1}\frac{1}{j^\alpha}. \tag{3.13}$$

If we consider the limit $N \to \infty$ we note

$$\lim_{N\to\infty}\sum_{j=1}^{N-1}\frac{1}{j^\alpha} \to \begin{cases} \infty, & \text{for } 0 \leq \alpha \leq 1, \\ k(\alpha), & \text{for } \alpha > 1, \end{cases} \tag{3.14}$$

where $k(\alpha)$ is a constant independent of N. We see that if we want the energy to scale as N, we need the scaling factor C_N to be constant in the short-range case. In the long-range case this scaling factor is a function of N which depends on the parameter α.

The exact α dependence of C_N in this case, as introduced in [20], can be computed in the

$N \to \infty$ limit which gives

$$C_N \sim \begin{cases} \frac{2^{\alpha-1}N^{1-\alpha}}{1-\alpha}, & \text{for } 0 \leq \alpha < 1, \\ \ln N, & \text{for } \alpha = 1, \\ \xi(\alpha), & \text{for } \alpha > 1, \end{cases} \tag{3.15}$$

where ξ is the Riemann zeta function. This scaling law is consistent with the definition of long-range interactions given earlier. When the interactions are long-range, we can classify the model as pseudo-extensive in terms of energy, i.e the model can be made extensive with the correct choice of scaling factor. In the short-range case, the model is extensive in terms of energy for a scaling factor that is independent of N.

CHAPTER 4
Non-equivalence of ensembles

For short-range systems ensemble equivalence holds in the thermodynamic limit as discussed in section 2.3. This is a property of systems that are additive and as shown in the previous section, systems with long-range interactions are not necessarily additive. In this chapter we will consider the relationship between the canonical free energy and the microcanonical entropy and more specifically how this relationship is dependent on the convexity properties of these thermodynamic potentials. To develop this idea, let us first consider the method of recovering the different thermodynamic potentials from one another.

4.1 The Legendre-Fenchel transform

Before we show the relation between the thermodynamic potentials, we should first properly define them. The microcanonical density of states for a N-particle system is given by

$$\Omega(u) = \int \delta(u - H_N(x))dx,$$

while the canonical partition function is given by

$$Z(\beta) = \int e^{\beta H_N(x)}dx.$$

From these function we can calculate the entropy, defined as

$$s_N(u) = \ln \Omega(u)$$

and the free energy, defined as

$$\phi_N(\beta) = \ln Z(\beta).$$

From these definitions of the microcanonical entropy, s, and the canonical free energy, ϕ, it is straightforward to show that the free energy is related to the entropy by

$$\phi_N(\beta) = -\frac{1}{N\beta} \ln \int d(Nu) \exp(-N[\beta u - s_N(u)]) \tag{4.1}$$

If we now consider the free energy in the thermodynamic limit, $N \to \infty$, this integral can be approximated by Laplace's method. This means that only the maximum of the exponent in the integration interval will give a notable contribution to the integral. The free energy in

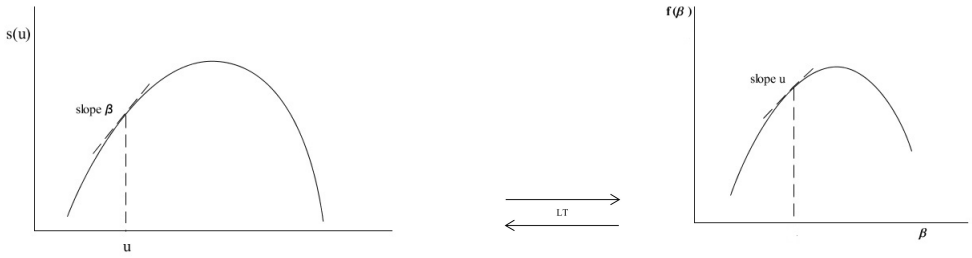

Figure 4.1: Graphic illustration of the Legendre transform. Since the entropy and free energy are strictly concave in the case where the entropy is a strictly concave, the Legendre transform is a mapping between the entropy and the free energy.

the thermodynamic limit is therefore given by

$$\beta\phi(\beta) = \inf_u\{\beta u - s(u)\} \tag{4.2}$$

This is known as the Legendre-Fenchel transform. The Legendre-Fenchel transform geometrically implies lowering a tangent with slope β onto the entropy curve and finding the u where the curve and the tangent first meet. This is graphically represented in figure 4.1. From this definition of the free energy it is clear that it is a concave function. It is tempting to try and recover the entropy by performing a Legendre-Fenchel transform of the free energy,

$$\beta s(u) \sim \inf_\beta\{\beta u - \phi(\beta)\}, \tag{4.3}$$

but as we will see in section 4.2 the entropy is not necessarily a concave function so that this would not, in general, yield the correct result.

4.2 Convexity properties of the thermodynamic potentials

In figure 4.1 both the free-energy and entropy are strictly concave functions and performing the Legendre transform recovers the correct function from the other. This is because the Legendre transform is a one-to-one mapping here between the function and its family of tangents at every point. Unfortunately this is not always the case.

Consider a system with long-range interactions that is not additive. The discussion in this section is similar to the discussion in [7]. In this scenario a non-concave entropy is physically realizable [7]. In figure 4.2 a non-concave entropy is shown. Note that if the system were additive, we could split the system in two, at the phase with energy u_1 and phase with energy

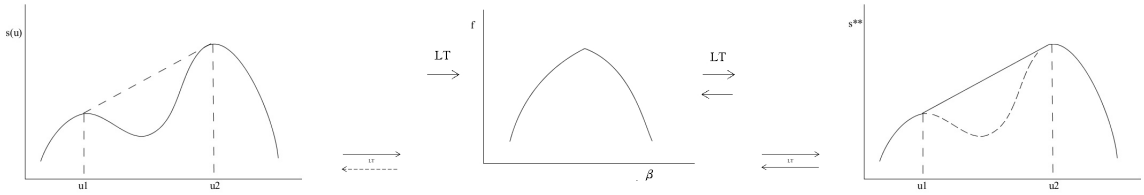

Figure 4.2: Non-concave entropy and the corresponding free energy recovered by the Legendre transform. The correct free energy is obtained by doing a Legendre transform of the entropy, but doing a Legendre transform of the free energy only recovers the concave envelope of the entropy. The states between u_1 and u_2 in the entropy are not correctly recovered from the free energy.

u_2, so that the energy between these phases will be given by the mixed phase,

$$u = ku_1 + (1-k)u_2, \tag{4.4}$$

where k is the fraction of the phase u_1 and $(1-k)$ is the fraction of phase u_2. Since the entropy is extensive and additive, it would then be the tangent between them (shown as the dotted line in figure 4.2). If the system were additive this splitting up would correspond to the correct entropy since it is maximal.

In the case of a non-concave entropy (solid line in figure 4.2) the correct free energy is still obtained from the Legendre transform in the thermodynamic limit since (4.2) is always valid, with the energy states between u_1 and u_2 being transformed to a single point β_t. This point will be a point of the free-energy function which corresponds to a discontinuous first derivative. Note here that doing the Legendre transform of the free-energy only recovers the concave envelope, s^{**}, of the entropy and that s and s^{**} are not the same [7].

At this stage it is useful to point out the properties of a system with a non-concave entropy, apart from the non-equivalence of the thermodynamic potentials.

4.3 Negative specific heat

Although it may seem counter intuitive, the specific heat of a system with long range interactions can be negative. This is counter intuitive in the sense that pumping energy into the system will lower the temperature. In self-gravitating systems, this usually coincides with a phase transition from a 'clustered' to a 'gas' phase [1]. The explanation as to how negative specific heat relates to non-equivalence of ensembles was first discussed by Thirring [12] who used the idea to account for the microcanonical negative specific heat found for self-gravitating gas spheres by Lynden-Bell and Wood [13].

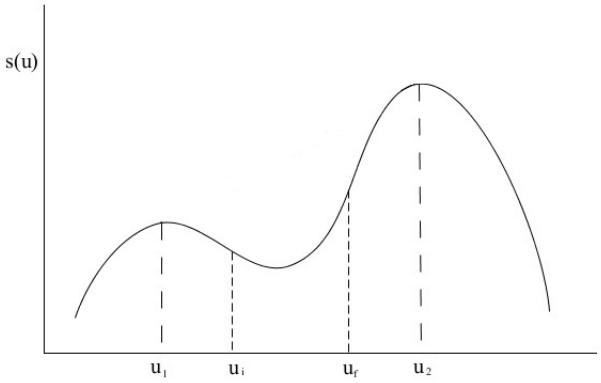

Figure 4.3: Non-concave entropy with the region of negative specific heat between u_i and u_f. Although the points between u_1 and u_2 correspond to the ensembles being non-equivalent, only the points between u_i and u_f correspond the negative specific heat since the curvature in this range is positive.

The curvature of the entropy as a function of energy is related to the heat capacity, C_v, and temperature, T, by

$$\frac{\partial^2 s}{\partial u^2} = -\frac{1}{C_v T^2} \tag{4.5}$$

Now if we consider the non-additive system with non-concave entropy in figure 4.3 we note that the curvature of s in the range $\{u_i, u_f\}$ is positive, $\partial^2 s/\partial u^2 > 0$, and since $T^2 > 0$ this implies that $C_v < 0$. This in turn implies that the specific heat $c_v = C_v/N$ is negative.

Here we see that the negative specific heat is a direct consequence of the non-concave entropy, which in turn is related to the non-additivity. However in the canonical ensemble the specific heat is given by

$$\frac{\partial^2 \phi}{\partial \beta^2} = -\frac{c_v}{T^2}, \tag{4.6}$$

where $\phi(\beta, n) = \beta f(\beta, n)$ is a concave function for fixed particle density n (in the thermodynamic limit). Therefore $c_v > 0$. The free-energy is always concave by definition.

4.4 Negative magnetic susceptibility

In the same way that the specific heat, c_v, describes the response of the temperature in terms of a change in energy, the magnetic susceptibility, χ, describes the response of the magnetisation, m, in terms of a change in magnetic field, h. We would therefore expect the magnetic susceptibility to be positive, so that the magnetization increases as the magnetic field is increased. For the canonical ensemble the magnetic susceptibility, given by

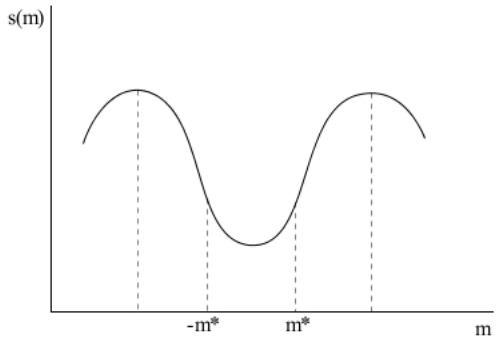

Figure 4.4: Non-concave entropy with the region of negative magnetic susceptibility between $-m*$ and $m*$. Note here we consider m to be the only conserved quantity so that the region of negative magnetic susceptibility is only determined by the curvature of s(m).

$$\chi(\beta, h) = \frac{\partial m(\beta, h)}{\partial h} \geq 0, \tag{4.7}$$

is always positive. The proof of this, as shown in [21], follows from rewriting the magnetic susceptibility as

$$\chi(\beta, h) = -\frac{1}{\beta}\frac{\partial^2 \phi(\beta, h)}{\partial h^2} \tag{4.8}$$

and by noting $\phi(\beta, h)$ is a convex function $\partial^2\phi(\beta, h)/\partial h^2 \leq 0$, so that $\chi(\beta, h) \geq 0$.

In the microcanonical ensemble this is not the case, here the proper magnetic susceptibility [21] to consider is

$$\chi(\epsilon, m) = \left(\frac{\partial h(\epsilon, m)}{\partial m}\right)^{-1} = \left(\frac{\partial s}{\partial \epsilon}\right)^2 \left(\frac{\partial^2 s}{\partial m \partial \epsilon}\frac{\partial s}{\partial m} - \frac{\partial s}{\partial \epsilon}\frac{\partial^2 s}{\partial m^2}\right)^{-1} \tag{4.9}$$

Note that the magnetic susceptibility is not only dependent on the curvature of the entropy in terms of the magnetisation, m. This is due to the fact that energy, ϵ, and magnetisation are conserved quantities. The same holds for the specific heat when the energy and magnetisation are conserved. Although it is not sufficient to determine the curvature of the entropy when making claims about the sign of the magnetic susceptibility, it is clear that the magnetic susceptibility in the microcanonical ensemble is dependent on the curvature in terms of internal energy, ϵ and magnetisation, m.

4.5 Macro state non-equivalence

In [22] Touchette proves, by following [23], that non-equivalence of the thermodynamics potentials also corresponds to macro state non-equivalence. Therefore the equilibrium states that are represented in the non-concave part of the entropy in figure 4.3, where $u_1 < u < u_2$, are not represented in the canonical ensemble. Consider the non-concave entropy in figure 4.3 again. We can split the domain of the entropy in two parts, namely when the energy is $u < u_1$ or $u > u_2$ and when the energy is $u_1 < u < u_2$. This corresponds to the domains where the entropy is concave and non-concave respectively. These two domains also represent the domains where there is macrostate equivalence and non-equivalence. There is also the special case when the entropy is affine. The entropy is affine in terms of the variable u when it can be represented as linear function in terms of u, $s(u) = Au + C$, where A and C are independent of u. In this case we say the macrostates are partially equivalent. This is because on the affine part of the entropy all the energy states transform to the same β. In figure 4.3 the points u_1 and u_2 transform to the same β since they have the same slope.

The physical meaning of non-equivalent macrostates is that if we were to prepare a long-range system experimentally where we fix the particle number and fix the **energy** to a value between u_1 and u_2 the system would equilibrate to a state that would not be present if we prepared the same system at any **temperature** with fixed particle number since there is not a one-to-one correspondence between the microcanonical and canonical macro states. This is the basis of the possible experimental verification of non-equivalence of ensembles.

4.6 Thermodynamic convexity in small systems

Before concluding this chapter, it is worthwhile mentioning that the entropy can also be non-concave for systems with short-range interactions close to a phase transition when doing numerical simulations. This is however a finite size effect and it has been shown that by increasing the system size, the convex part of the entropy approaches the concave envelope of the convex part [24]. Therefore in small systems one has to be careful when talking about non-equivalent ensembles because a non-concave entropy may well be just the signature of a first-order phase transition, or might even disappear in the thermodynamic limit without a phase transition occurring.

In [25], Gross proposes the following set of signatures for phase transitions of **small** systems in the microcanonical ensemble, that will be used throughout this thesis in the context of infinite systems.

(1) A single stable phase if the curvature is positive (strictly concave).
(2) First order phase transition if there is a region where the curvature is negative ('convex intruder').
(3) Second order phase transition if there is a line (for which the curvature is zero) where two neighbouring phases become indistinguishable.

As discussed earlier, signature 2 corresponds to non-equivalent ensembles if the 'convex intruder' remains convex in the thermodynamic limit. If this 'convex intruder' is simply the sign of a phase transition or a finite size effect, it would converge to an affine region or disappear in the thermodynamic limit. It should also be remarked that these signatures of phase transitions are only valid for the curvature of the entropy in terms of extensive parameters.

CHAPTER 5
Experimental realization

Experimentally confirming non-equivalence of ensembles would mean preparing a model in a microcanonical setting and verifying the existence of an equilibrium macrostate that does not have a corresponding canonical macro state. Ideally the model we would like to prepare in a microcanonical setting, should be analytically solvable. In this case, the comparison of the experimental and analytical results would be possible. Following the suggestions in [26], a promising model in this regard is the anisotropic Heisenberg model, which will be discussed in chapter 6. Historically the anisotropic Heisenberg model was used to explain the behaviour of spin chains connected to a heat bath, so that it should be treated in the canonical ensemble. Recently it has been shown that this model can be engineered with cold atoms in an optical lattice [27]. In this chapter we will first mention these optical lattices and then look at the proposed possibilities of engineering long-range interactions and measuring the appropriate parameters.

5.1 Cold atoms in optical lattices

Optical lattices consist of counter-propagating laser beams, creating a periodic potential that can trap neutral particles at fixed lattice sites. When these particles are cooled they congregate to the periodic potential minima which causes a crystal lattice like-structure, see figure 5.1. Here the neutral particles are, for instance, analogous to electrons in naturally occurring crystals. Studying optical lattices has two substantial advantages over studying naturally occurring crystals or other condensed matter systems. Firstly these optical lattices do not have the imperfections that occur in natural crystals and secondly the interactions between particles are highly controllable. These optical lattices are therefore ideal 'quantum simulators' for studying condensed matter systems. After cooling these optical lattices the particle number, energy and for certain cases the magnetisation are well conserved. The appropriate setting is therefore the microcanonical one.

5.1.1 Long-range interactions

In [27], Micheli et al. show that using cold atoms or molecules with permanent electric or magnetic dipole moments results in dipole-dipole interaction that decay with inter particle distance as $1/r^3$. They also show that a model similar in nature to the one we will be considering in chapter 6 can be engineered in these optical lattices. Alternatively, as shown

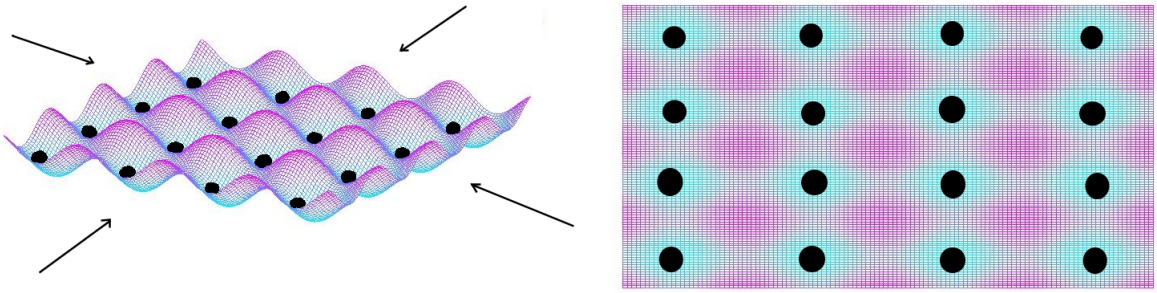

Figure 5.1: Illustration of a optical lattice with particles trapped by counter-propagating laser beams creating a periodic potential. The figure on the right shows the top view of the lattice structure.

in [28], interactions of a $1/r$ type can be achieved by inducing a dipole moment in atoms that do not have a permanent dipole moment. Unfortunately with dipole-dipole interactions, magnetisation is not conserved, which limits the verification of non-equivalence of ensembles to trying to observe energy states that do not have corresponding temperature states.

5.2 Measurements

In the proposed experiments mentioned in section 5.1.1, the magnetisation is not a conserved quantity under time evolution. This means that the magnetisation will not in general approach an equilibrium value so that it is not a useful quantity to characterise an equilibrium state, since it will fluctuate. To circumvent this problem we could either map the spin model to a lattice gas model, or we could maximize the entropy in terms of magnetisation so that we only have the entropy in terms of energy. The latter of these options is discussed in section 9.3. If we map the spin model to a lattice gas model, the magnetisation is mapped to particle density. In optical lattice experiments particle density is well conserved. The lattice gas equivalent to magnetic susceptibility is compressibility. Although this was not mentioned in chapter 4, the compressibility can be negative for the microcanonical ensemble and this also corresponds to non-equivalence of ensembles. An example of this is given in [29].

In section 2.2 we briefly mentioned the existence of quasi-stationary states in systems with long-range interactions. This property can be an experimental obstacle, since we are interested in measuring the energy and magnetisation of equilibrium states and not quasi-stationary states. The optical lattice must therefore be kept intact longer than the equilibration time needed for the system which, for long-range systems, might diverge with system size.

CHAPTER 6
Model

In light of the discussion in chapter 5, we have a model that looks appropriate to experimentally study non-equivalence of ensembles. In this chapter we will introduce this model and the necessary assumption needed to make it analytically solvable.

6.1 The Curie-Weiss anisotropic quantum Heisenberg model

The model we are considering consists of N spin-1/2 particles, interacting via Curie-Weiss type interactions. This means that each particle interacts with each of the other $N-1$ particles at equal strength. The particles are also in the presence of an external magnetic field, $\underline{h}$, orientated in an arbitrary direction. $\underline{h}$ consists of the components h_1,h_2 and h_3 in the x,y and z directions respectively. The Hamiltonian of this system is given by

$$H_h = -\frac{1}{2N}\sum_{k,l=1}^{N}(\lambda_1\sigma_k^1\sigma_l^1 + \lambda_2\sigma_k^2\sigma_l^2 + \lambda_3\sigma_k^3\sigma_l^3) - \underline{h}\cdot\sum_{k=1}^{N}\underline{\sigma}_k, \tag{6.1}$$

where σ_k^i is the i^{th} component Pauli spin-1/2 operator acting on the k^{th} factor of the tensor product of N copies of the spin -1/2 Hilbert space. The constants λ_1,λ_2 and λ_3 act as the coupling constants in the x,y and z directions respectively. These coupling constants are non-negative for the ferromagnetic case.

For the sake of convenience we can use the commonly adopted notation of writing the σ operators as collective spin operators defined by

$$S_i = \frac{1}{2}\sum_{j=1}^{N}\sigma_j^i, \tag{6.2}$$

with $i \in \{1,2,3\}$. The Hamiltonian can now be written as

$$H_h = -\frac{2}{N}(\lambda_1 S_1^2 + \lambda_2 S_2^2 + \lambda_3 S_3^2) - 2\underline{h}\cdot\underline{S} \tag{6.3}$$

6.2 Special values of the coupling constants

For certain values of the coupling constants the model reduces to important well known cases. Firstly, when $\lambda_1 = \lambda_2 = \lambda_3$, it yields the isotropic Heisenberg model. When $\lambda_1 = \lambda_2$ and $\lambda_3 = 0$, it gives the Lipkin-Glick model (otherwise known as the XY-model). Finally

when $\lambda_1 = \lambda_2 = 0$ it gives the Ising model. In [26], Kastner shows that in these cases (i.e. $\lambda_1 = \lambda_2$), if the magnetic field is pointing in the z-direction, the Hamiltonian can be expressed entirely in terms of the operators $\mathbf{S}^2$ and S_3 so the model can be solved by straightforward means. Additionally the exact expression for the canonical free energy for this model has been computed [5], so that comparing results between the canonical and microcanonical cases is possible.

6.3 Curie-Weiss type interactions

The choice of the Curie-Weiss type interactions is responsible for making the model analytically solvable (see chapter 7). Although the Curie-Weiss type interactions cannot be simulated in optical lattice experiments, it is well known that these type of interactions can be seen as the limiting case of long-range interactions and that they exhibit much of the same characteristics in terms of phase transitions [30] [31]. Thus we are well justified in thinking that if we have regions of negative specific heat or magnetic susceptibility for the model with Curie-Weiss type interaction it may indeed also appear for the systems with interaction potential decaying as $1/r^3$ or $1/r$ that can be engineered in optical lattices.

CHAPTER 7
Microcanonical entropy

In this chapter we will discuss the formulation for the entropy in terms of internal energy, ϵ, and magnetisation, $\underline{m}$. From the entropy, $s(\epsilon, \underline{m})$, we can recover the free energy as a function of inverse temperature, β, and magnetic field, h. The entropy in terms of internal energy and magnetisation also contains the necessary information to recover the entropy in terms of external magnetic field, h, and total energy, u, which will be done in section 9.3. After we have formulated the entropy, we show that we can write this expression for the entropy in an appropriate form that can be solved by asymptotic evaluation in the thermodynamic limit.

7.1 Formulation

If we want to compute the density of states for a state with energy ϵ and magnetisation $\underline{m}$, it is as simple as counting number of states, x, with energy $\bar{\epsilon}(x) = \epsilon$, and $\underline{\bar{m}}(x) = \underline{m}$. Mathematically this is represented as

$$\Omega_{classical}(\epsilon, \underline{m}) = \sum_x \delta_\Delta(\bar{\epsilon}(x) - \epsilon)\delta_\Delta(\underline{\bar{m}}(x) - \underline{m}), \tag{7.1}$$

where the summation is over phase space and $\bar{\epsilon}(x)$, and $\underline{\bar{m}}(x)$ are phase space functions. For simplicity we assume the phase space is discrete. Here we see that if we pick a state with energy $\bar{\epsilon}(x) \in [\epsilon - \Delta, \epsilon]$ and $\underline{\bar{m}}(x)$ is in the interval $[\underline{m} - \Delta, \underline{m}]$ we add one to the sum. The Δ's are small but arbitrary positive constants which can be seen as achievable experimental resolution when measuring the energy and magnetisation. This regularisation also avoids mathematical problems with delta functions. Consider that in the thermodynamic limit the number of allowed energy states will be dense, so that for instance we can find a value of the phase space function, $\bar{\epsilon}(x)$ arbitrarily close to an allowed state ϵ for some x. But the phase space functions do not necessarily have rational values. Now since there are infinitely many real numbers (an uncountable set) on any interval on the real line and rational numbers are a countable subset of these numbers, the density of states will be zero almost everywhere. This problem is easily solved by adding an arbitrarily small delta regularisation.

When we consider quantum systems, the operators H_0 and M will in general not commute and therefore an eigenvalue of H_0 will not have a unique corresponding eigenvalue of M. So if you measure the magnetisation corresponding to the eigenvalue $\bar{\epsilon}$, you can get a number of possible values of $\underline{\bar{m}}$, each with a certain probability. For one-dimensional subspaces, this

probability is given by the overlap $|\langle\bar{\epsilon}|\underline{\bar{m}}\rangle|^2$. So how can we then define a physically reasonable density of states? One suggestion is to pick an eigenvalue $\bar{\epsilon}$ and sum up all the probabilities for finding an eigenvalue $\underline{\bar{m}}$. This is the idea behind the suggestion made by Truong [9] and the corresponding density of states is then given by

$$\Omega_N(\epsilon, \underline{m}) = \sum_{\bar{\epsilon}, \underline{\bar{m}}} Tr[P_{H_0}(\bar{\epsilon}) P_M(\bar{m})] \delta_\Delta(\bar{\epsilon} - \epsilon) \delta_\Delta(\underline{\bar{m}} - \underline{m}), \tag{7.2}$$

where $P_{H_0}(\bar{\epsilon})$ and $P_M(\bar{m})$ are the eigenprojections of the operators H_0 and M with eigenvalues ϵ and $\underline{m}$ respectively. The trace and eigenprojection formulation used here is the higher dimensional equivalent to the overlap mentioned previously, therefore it gives the probability of measuring an eigenvalue of $\bar{\epsilon}$ if given an eigenvalue of $\underline{\bar{m}}$. The corresponding entropy is then given by

$$s_N(\epsilon, \underline{m}) = \frac{1}{N} \ln \Omega_N(\epsilon, \underline{m}). \tag{7.3}$$

This entropy does not describe a system with fixed energy and magnetisation for finite systems since, as discussed earlier, the uncertainty principle resulting from the non-commuting operators does not allow fixed values of ϵ and m. Our hope is however that in the thermodynamic limit, $N \to \infty$, the corrections due to the commutators will vanish and the entropy will converge to the description of a system with fixed energy ϵ and magnetisation $\underline{m}$.

Although the formulation of the entropy described in (7.2) is intuitive, it is hard to compute mathematically. Instead we will assume that in the large N-limit the operators commute and therefore the eigenprojections in (7.2) are equal to one. We will also not implement the Δ-regularisation as used in the formulation and use unregularised Dirac delta functions and later perform a mathematical trick to impose an artificial regularisation. The density of states without this regularisation is then given by

$$\Omega_N(\epsilon, \underline{m}) = Tr\left[\delta(\epsilon - \frac{H_0}{N}) \delta(m_1 - \frac{M_1}{N}) \delta(m_2 - \frac{M_2}{N}) \delta(m_3 - \frac{M_3}{N})\right]. \tag{7.4}$$

Note that in line with the argument about delta regularisation, this expression does not mathematically make sense since the density of states will be zero almost everywhere. Now if we insert the factors $\exp[a(N\epsilon - H_0)]$, $\exp[b_1(Nm_1 - M_1)]$, $\exp[b_2(Nm_2 - M_2)]$ and $\exp[b_3(Nm_3 - M_3)]$ in the trace the value of the density of states remains the same. This technique was inspired by [26]. Combining these terms in the exponential and expressing the delta's in their

Fourier representation leads us to

$$\Omega_N(\epsilon, \underline{m}) = \frac{N^4}{(2\pi)^4} Tr \int_{-\infty}^{\infty} dk \int_{-\infty}^{\infty} d^3l \left[\exp[(a+ik)(N\epsilon - H_0)] \prod_{j=1}^{3} \exp[(b_j + il_j)(Nm_j - M_j)] \right]. \tag{7.5}$$

This expression is still not well defined and in order to recover an expression that is reasonable we now want to impose some artificial delta regularisation. Although this will not make sense at the moment, consider the expression for the density of states above with the trace being evaluated before the integration is performed

$$\Omega_N(\epsilon, \underline{m}) = \frac{N^4}{(2\pi)^4} \int_{-\infty}^{\infty} dk \int_{-\infty}^{\infty} d^3l Tr \left[exp[(a+ik)(N\epsilon - H_0)] \prod_{j=1}^{3} exp[(b_j + il_j)(Nm_j - M_j)] \right]. \tag{7.6}$$

We claim that this imposes an artificial regularisation on the delta functions and that this expression is mathematically well defined. To justify this I will not give any rigorous proof but rather show that calculating the density of states in another manner will lead to the same result.

7.2 Inverse Laplace transform

It is well known that the density of states can be computed by doing an inverse Laplace transform of the canonical partition function. When doing the resulting integral in the large N limit we have to be careful, because as shown in [32] if only the leading order terms are considered this may lead to recovering only the concave envelope of the entropy. Touchette does however show that this method is a viable option to calculate a non-concave entropy if the integral in the large N limit is done properly. Consider the partition function,

$$Z_N(\beta, \underline{h}) = Tre^{-\beta(H_0 - \underline{h}\cdot\underline{M})}, \tag{7.7}$$

now computing the inverse Laplace-transform by using Mellin's inverse formula [33],

$$L^{-1}\{F(s)\} = f(t) = \frac{1}{2\pi i} \lim_{T\to\infty} \int_{a-iT}^{a+iT} e^{st} F(s) ds,$$

where $a = Re(s)$, gives

$$\Omega_N(\epsilon, \underline{m}) = L^{-1}\{Z(\beta, \underline{h})\}$$

$$
\begin{aligned}
&= \frac{1}{(2\pi i)^4}\int_{a-i\infty}^{a+i\infty} d(N\beta)e^{N\beta\epsilon}\int_{\underline{b}-i\infty}^{\underline{b}+i\infty} d^3(-N\beta h)e^{-N\beta\underline{h}\cdot\underline{m}}Tr\left[e^{-\beta H_0+\beta\underline{h}\cdot\underline{M}}\right]\\
&= \frac{-N^4}{(2\pi)^4}\int_{a-i\infty}^{a+i\infty} d(\beta)\int_{b-i\infty}^{b+i\infty} d^3(\tilde{h})Tr\{\exp\left[\beta(N\epsilon-H_0)+\tilde{\underline{h}}\cdot(N\underline{m}-\underline{M})\right]\} \qquad (7.8)\\
&= \frac{N^4}{(2\pi)^4}\int_{-\infty}^{\infty} dk\int_{-\infty}^{\infty} d^3lTr\left\{\exp\left[(a+ik)(N\epsilon-H_0)+\sum_{j=1}^{3}(b_j+il_j)(Nm_j-M_j)\right]\right\}.
\end{aligned}
$$

This expression for the density of states is equivalent to the density of states derived earlier rather crudely if the operators H_0 and M_j, $j\in\{1,2,3\}$ commute in the large N limit. The regularisation imposed therefore yields a density of states that is well defined.

Although these formulations of the density of states are constructed from different bases, they are completely equivalent. By considering the suggestion made by Truong however, we are given a physical way to think about the formulation of the density of states in terms of non-commuting operators.

7.3 Calculating the entropy

In order to evaluate expression (7.8) for the Hamiltonian (6.1), we need to rewrite the density of states so that the N-spin trace is decoupled into the product of one-spin traces. This method was used similarly in [26] and inspired by [34] for the general canonical case.

The density of states is given by

$$
\Omega_N(\epsilon,\underline{m}) = \frac{N^4}{(2\pi)^4}\int_{-\infty}^{\infty} dk\int_{-\infty}^{\infty} d^3lTr\left[\exp[(a+ik)(N\epsilon+\frac{2}{N}\sum_{j=1}^{3}\lambda_j S_j^2)]\prod_{j=1}^{3} exp[(b_j+il_j)(Nm_j-2S_j)]\right]. \qquad (7.9)
$$

We can rewrite the first exponential in the trace by using the Lie-Trotter formula, proved in [35], which is given by

$$
e^{A+B} = \lim_{N\to\infty}\left(e^{\frac{A}{N}}e^{\frac{B}{N}}\right)^N,
$$

so that this gives

$$
\exp[(a+ik)(N\epsilon+\frac{2}{N}\sum_{j=1}^{3}\lambda_j S_j^2)] = \lim_{n\to\infty}\left[exp\left(\frac{(a+ik)N\epsilon}{n}\right)\prod_{\alpha=1}^{3} exp\left(\frac{2(a+ik)}{nN}\lambda_\alpha S_\alpha^2\right)\right]^n. \qquad (7.10)
$$

We can now use the Hubbard-Statonovich trick to linearise the exponential in terms of the operator S_j. This is the crucial part necessary to decouple the trace into the product of

one-spin traces. For a constant, c, with positive real part and an operator, S, the Hubbard-Stratonovich trick [36] [37] enables us to rewrite

$$e^{cS^2} = \frac{1}{n\sqrt{\pi c}} \int dx \exp\left(\frac{-x^2}{cn^2}\right) \exp\left(\frac{2xS}{n}\right). \tag{7.11}$$

Using this in (7.10) gives

$$\lim_{n\to\infty} \left[\frac{N}{2\pi n(a+ik)} \exp\left(\frac{(a+ik)N\epsilon}{n}\right) \int d^3x \exp\left(-\frac{n\underline{x}\cdot\underline{x}}{2n(a+ik)}\right) \prod_{\alpha=1}^{3} \exp\left(\frac{2x_\alpha\sqrt{\lambda_\alpha}S_\alpha}{n}\right)\right]^n, \tag{7.12}$$

where $x = (x_1, x_2, x_3)$. Now we want to make the replacement

$$\prod_{\alpha=1}^{3} \exp\left(\frac{2x_\alpha\sqrt{\lambda_\alpha}S_\alpha}{n}\right) = \exp\left(\frac{2}{n}\sum_{\alpha=1}^{3} x_\alpha\sqrt{\lambda_\alpha}S_\alpha\right). \tag{7.13}$$

The equality sign here is of course in general not true since the operators in the exponent do not necessarily commute, but the corrections given by the Baker-Campbell-Hausdorff formula are of the order $\frac{1}{n^2}$ and higher so since we are considering this in the $n \to \infty$ limit the corrections are considered negligible, so that (7.13) becomes

$$\prod_{\alpha=1}^{3} \exp\left(\frac{2x_\alpha\sqrt{\lambda_\alpha}S_\alpha}{n}\right) = \exp\left(-\frac{1}{n}\sum_{i=1}^{N}\phi_i(\underline{x})\right) \tag{7.14}$$

$$= \prod_{i=1}^{N} \exp\left(-\frac{\phi_i(\underline{x})}{n}\right), \tag{7.15}$$

with

$$\phi_i(\underline{x}) = -\sum_{\alpha=1}^{3} x_\alpha\sqrt{\lambda_\alpha}\sigma_i^\alpha. \tag{7.16}$$

Here we do not have a problem with replacing the sum in the exponential with a product of exponentials since $\phi_i(\underline{x})$ and $\phi_j(\underline{y})$ consist of one-spin operators acting on different factors of the tensor product Hilbert space, therefore they must commute when $i \neq j$.

Now using this in (7.12) we have

$$\lim_{n\to\infty} \left[\frac{N}{2\pi n(a+ik)} \exp\left(\frac{(a+ik)N\epsilon}{n}\right) \int d^3x \exp\left(-\frac{n\underline{x}\cdot\underline{x}}{2n(a+ik)}\right) \prod_{i=1}^{N} \exp\left(-\frac{\phi_i(\underline{x})}{n}\right)\right]^n. \tag{7.17}$$

We can substitute this expression into the density of states together with the substitutions

$s = a + ik$ and $r_j = b_j + il_j$, this gives

$$\begin{aligned}\Omega_N(\epsilon, \underline{m}) &= \lim_{n\to\infty} \frac{N^4}{(2\pi)^4} \int_{a-i\infty}^{a+i\infty} ds e^{N\epsilon s} \int_{\underline{b}-i\infty}^{\underline{b}+i\infty} d^3 r e^{N\underline{r}\cdot\underline{m}} \left(\frac{N}{2\pi n s}\right)^{\frac{3n}{2}} \\ &\times \int \cdots \int d^3x^{(1)} \cdots d^3x^{(n)} \exp\left(-\frac{N}{2ns} \sum_{m=1}^{n} \underline{x}^{(m)} \cdot \underline{x}^{(m)}\right) \\ &\times Tr\left[\prod_{m=1}^{n}\prod_{i=1}^{N} \exp\left(-\frac{\phi_i(\underline{x}^{(m)})}{n}\right) \prod_{j=1}^{3} \exp(-2r_i S_i)\right]. \end{aligned} \tag{7.18}$$

Here we have used the linearity property of the trace. Note that the trace in (7.18) only acts on the exponentials of one-particle operators. We can therefore rewrite this trace on the N-spin Hilbert space as the product of traces tr_q over one-spin Hilbert spaces, where q labels the different one-spin Hilbert spaces. The two operators in the exponents of the trace again do not in general commute but, as discussed earlier, the corrections will disappear in the $n \to \infty$ limit so that we can write the trace as

$$Tr\left\{\prod_{q=1}^{N}\prod_{m=1}^{n} \exp\left[-\frac{1}{n}\left(\phi_q(\underline{x}^{(m)}) + \sum_{j=1}^{3} r_j \sigma_q^j\right)\right]\right\}$$

$$= \prod_{q=1}^{N} tr_q \left\{\prod_{m=1}^{n} \exp\left[-\frac{1}{n}\left(\phi_q(\underline{x}^{(m)}) + \sum_{j=1}^{3} r_j \sigma_q^j\right)\right]\right\}.$$

Now the trace is decoupled as a product of one-spin traces and this trace can be computed. If we insert the expression for $\phi_q(\underline{x})$ and as before consider the corrections to the commutator as negligible, we get

$$\prod_{q=1}^{N} tr_q \left\{\exp\left[\frac{1}{n}\sum_{m=1}^{n}\sum_{\alpha=1}^{3}(x_\alpha^{(m)}\sqrt{\lambda_\alpha} - r_\alpha)\sigma_q^\alpha\right]\right\}.$$

Define the function

$$c_\alpha(\{x_\alpha^{(m)}\}, r_\alpha) = \frac{1}{n}\sum_{m=1}^{n}(x_\alpha^{(\underline{m})}\sqrt{\lambda_\alpha} - r_\alpha). \tag{7.19}$$

The expression for the trace is then finally

$$\prod_{q=1}^{N} tr_q \left\{\exp\left[\sum_{\alpha=1}^{3} c_\alpha \sigma_q^\alpha\right]\right\} = \prod_{q=1}^{N} tr_q \left[\exp\begin{pmatrix} c_3 & c_1 - ic_2 \\ c1 + ic_2 & -c_3 \end{pmatrix}\right]$$

$$= \left[tr \begin{pmatrix} e^{a} & 0 \\ 0 & e^{-a} \end{pmatrix} \right]^{N} = [2cosh(a)]^{N}, \tag{7.20}$$

with $a(\{\underline{x}^{(m)}\}, \underline{r}) = \sqrt{c_1^2 + c_2^2 + c_3^2}$. Substituting this into the density of states (7.18), yields

$$\begin{aligned} \Omega_N(\epsilon, \underline{m}) &= \lim_{n\to\infty} \frac{2^N N^4}{(2\pi)^4} \int_{a-i\infty}^{a+i\infty} ds \int_{\underline{b}-i\infty}^{\underline{b}+i\infty} d^3r \left(\frac{N}{2\pi n s}\right)^{\frac{3n}{2}} \\ &\times \int \cdots \int \prod_{m=1}^{n} d^3x^{(m)} \exp\left[N F(s, \underline{r}, \{\underline{x}^{(m)}\}) \right], \end{aligned} \tag{7.21}$$

with

$$F(s, \underline{r}, \{\underline{x}^{(m)}\}) = \epsilon s + \underline{r} \cdot \underline{m} - \frac{1}{2ns} \sum_{m=1}^{n} \underline{x}^{(m)} \cdot \underline{x}^{(m)} + \ln[\cosh(a(\{\underline{x}^{(m)}\}, \underline{r}))]. \tag{7.22}$$

CHAPTER 8
Asymptotic evaluation of integral

Following chapter 7 the expression for the density of states is in a form that can be solved by asymptotic evaluation, since we will use the density of states to evaluate the entropy in the $N \to \infty$ limit. For a textbook discussion on the asymptotic evaluation of integrals we refer the reader to [38]. In sections 8.1 and 8.2 we will introduce two methods that seem applicable and discuss the possible pitfalls these methods might have in the microcanonical setting. In section 8.3 we will proceed to calculate the entropy in the appropriate manner.

8.1 Method of steepest descent

Consider an integral of the form

$$I(s,t) = \int_C ds \int_{\tilde{C}} dt e^{NZ(s,t)}, \tag{8.1}$$

where N is a large parameter, s and t are complex variables and C and $\tilde{C}$ are the contours of integration in the complex plane. If we assume the function Z is analytic, we can split it into two real valued analytic functions g and h of s and t so that

$$Z(s,t) = g(s,t) + ih(s,t). \tag{8.2}$$

For non-constant h, this exponential function is rapidly oscillating in the large N limit, so that the contributions to the integral are canceled by consecutive oscillations and only the parts where the integral is not oscillating rapidly gives meaningful contributions to the integral. The idea behind the method of steepest descent is to use the analyticity of the functions g and h to deform the contour of integration into contours, C' and $\tilde{C}'$, where h is constant (and where the function is not oscillating rapidly), so that $Z(s,t) = g(s,t) + ih$ and

$$I(s,t) = e^{iNh} \int_{C'} ds \int_{\tilde{C}'} dt e^{Ng(s,t)}. \tag{8.3}$$

Because the function g is real, the remaining integral can be solved in the large N limit by Laplace's method which implies that

$$I(s,t) \cong e^{iNh} e^{Ng(s_0,t_0)}, \tag{8.4}$$

where s_0 and t_0 are the values of s and t at the absolute minimum of g on the contours C' and $\tilde{C}'$. In the above equations the approximation is exact in the N to infinity limit. Using this for the integral we have for the density of states (7.21), it is clear that it can be solved by deforming the s, $\underline{r}$ and $\{\underline{x}^{(m)}\}$ integration paths so that the integration path corresponds to a constant imaginary part of F and then finding the maximum of the real part of F on that specific integration path. Specifically in this case since we know the entropy has to be a positive real valued function, the value of the imaginary part of F at this maximum has to be zero. But notice that the function $F(s, \underline{r}, \{\underline{x}^{(m)}\})$ is not analytic on the whole integration interval (i.e at $s = 0$ or $a = \pm\frac{i\pi}{2}$). So we have to consider an interval where the function is analytic and look for a maximum of the real part of F in that interval. In general it is not necessary for the real part of the function to have a single maximum, but nevertheless we have to choose one of the maxima and hope that either this is the only maximum or that this is the absolute maximum. In most cases not much attention is paid to this and the justification of the choice is usually based on the validity of the final solution obtained for the entropy. An example of this is given in [39], where the author simply shows that the exponent has a maximum in a certain interval for purely real values of the complex integration variables and then evaluates the exponent at this maximum. Before we implement this method it may be worthwhile to look at another possible way to solve this integral that is mathematically more rigorous, since the above method leaves some room for doubt.

8.2 Convergence of bounds in thermodynamic limit

In [34], Tindemans and Capel show that one can compute the free energy for systems with separable interactions in the canonical ensemble by proving that a particular choice of stationary point will lead to the correct result. To discuss this method and its applicability to the case we are studying, observe the integral obtained for the partition function in the canonical case after performing much the same steps we did in section 7.3

$$Z = \left(\frac{N}{2\pi n}\right)^{\frac{3n}{2}} \int_{-\infty}^{\infty} \cdots \int_{-\infty}^{\infty} \prod_{i=1}^{n} d^3x^{(i)} e^{NG(\{\underline{x}^{(i)}\})}. \tag{8.5}$$

The method described above consists of proving three parts namely,

1. For a particular stationary point $(\{x^{(m)}\}) = (\{x^0\})$ for all m,

$$G(\{x^0\}) = G_0, \tag{8.6}$$

where G_0 is the absolute maximum of the real part of G.

2. $f_\infty \leq G_0$,
3. $f_\infty \geq G_0$,

where f_∞ is the free energy in the thermodynamic limit,

$$f_\infty = \lim_{N\to\infty} \frac{1}{N} \ln Z. \tag{8.7}$$

From 2 and 3 it follows that $f_\infty = G_0$ and therefore that the stationary point in 1 is the correct one. Note that the first part of the proof is only valid if the imaginary part of the function G is zero at the stationary point, $G_2(\{x^0\}) = 0$. It also implies that the absolute minimum of the real part of G is at a stationary point of G, $\left(\partial G_2/\partial x^{(m)}\right)_{min} = 0$. The expression in (8.5) looks identical to the last $3n$ integrals in the expression for the density of states in the microcanonical case (7.21), so that it seems like this method could be applied.

8.2.1 Microcanonical ensemble

Consider expression (7.21) for the density of states,

$$\begin{aligned} \Omega_N(\epsilon, \underline{m}) &= \lim_{n\to\infty} \frac{2^N N^4}{(2\pi)^4} \int_{a-i\infty}^{a+i\infty} ds \int_{\underline{b}-i\infty}^{\underline{b}+i\infty} d^3r \left(\frac{N}{2\pi n s}\right)^{\frac{3n}{2}} \\ &\times \int \cdots \int \prod_{m=1}^{n} d^3x^{(m)} \exp\left[NF(s, \underline{r}, \{\underline{x}^{(m)}\})\right]. \end{aligned} \tag{8.8}$$

To use the method described in section 8.2, we need to show,

(a) that at a certain stationary point $(\underline{x}^{(m)}, \underline{r}, s) = (\underline{x}_0, \underline{r}_0, s_0)$ for all m,

$$F(\underline{x}_0, \underline{r}_0, s_0) = F_0, \tag{8.9}$$

where F_0 is the absolute maximum of the real part of F in (7.21).

(b) $s_\infty \leq F_0$,
(c) $s_\infty \geq F_0$,

where s_∞ is the entropy in the thermodynamic limit,

$$s_\infty = \lim_{N\to\infty} \frac{1}{N} \ln \Omega. \tag{8.10}$$

Before we proceed to implement this method we should remark on the differences between the two ensembles here. The integral for the partition function has $3n$ real integration variables whereas the integral for the density of states has $3n$ real and 4 complex integration variables. Also the function G in (8.5) is a analytic real valued function for all $x^{(i)}$ whereas the function F in (7.21) is not a real valued function in general and is not analytic on the whole integration interval.

8.2.2 (a) Absolute maximum of the real part of F

Following the canonical calculation in [34], we need to construct a function $\tilde{F}$,

$$\tilde{F}(\underline{x}^{(m)}, \underline{r}, s) = \frac{1}{n} \sum_{m=1}^{n} \phi(\underline{x}^{(m)}, \underline{r}, s), \tag{8.11}$$

which has the following properties:

$$\tilde{F} \geq F_1 \tag{8.12}$$

and

$$\tilde{F} = F_1 \text{ iff } (\underline{x}^{(m)}, \underline{r}, s) = (\underline{x}_0, \underline{r}_0, s_0), \tag{8.13}$$

where $(\underline{x}_0, \underline{r}_0, s_0)$ is the point where $\tilde{F}$ has a maximum. The function $\tilde{F}$ is therefore always larger than F_1, except at the point, $(\underline{x}_0, \underline{r}_0, s_0)$, where $\tilde{F}$ is maximal. Therefore F_1 has an absolute maximum at this point. This function can be constructed by using Hölder's inequality [40] and the proof of (8.11) and (8.12) can be done in the same manner as the canonical case, with the exception that the function F_1 is not analytic on the whole integration interval. So we can at best prove the existence of $\tilde{F}$ on certain subintervals of the integration interval. Although this is an inconvenience it is not the biggest problem in the microcanonical case. It is crucial to note that we cannot prove that

$$F_2(\underline{x}_0, \underline{r}_0, s_0) = 0, \tag{8.14}$$

$$\left(\frac{\partial F_2}{\partial x_i^{(m)}}\right)_{x_0} = \left(\frac{\partial F_2}{\partial r_i}\right)_{r_0} = \left(\frac{\partial F_2}{\partial s}\right)_{s_0} = 0, \tag{8.15}$$

at the point $(\underline{x}_0, \underline{r}_0, s_0)$ where F_2 is the complex part of F so that $F = F_1 + iF_2$. We require (8.14) since we know the entropy in the thermodynamic limit has to be a positive real valued function. From (8.15) we see that the absolute maximum of the real part of F is not necessarily a stationary point of F and, as discussed in section 8.1, the integral in (8.8) will be rapidly oscillating so that F_0 would give no contribution to the integral.

The reason why these properties cannot be proved for the microcanonical case is because of the additional 4 complex integration variables. In the canonical case these two properties follow immediately from (8.12) and (8.13).

Although we cannot prove (a), we hope that if we could prove (b) and (c) we could somehow circumvent the problem.

8.2.3 (b) Upper bound for the entropy

The upper bound for the entropy can be computed in much the same way as in the canonical case. To do this we use the fact that the density of states has to be a positive real valued function (and therefore the entropy is a positive, real valued function) together with the inequality

$$\left| \int_a^b f(x)dx \right| \leq \int_a^b |f(x)|\, dx, \tag{8.16}$$

to get a bound for the density of states

$$\begin{aligned}
\Omega_N(\epsilon, \underline{m}) &\leq \lim_{n\to\infty} \frac{2^N N^4}{(2\pi)^4} \int ds \int d^3r \left(\frac{N}{2\pi n(a^2+k^2)} \right)^{\frac{3n}{2}} \int \cdots \int \prod_{m=1}^{n} d^3x^{(m)} \left| e^{NF(s,\underline{r},\{\underline{x}^{(m)}\})} \right| \\
&= \lim_{n\to\infty} \frac{2^N N^2}{(2\pi)^4} \int ds \int d^3r \left(\frac{N}{2\pi n(a^2+k^2)} \right)^{\frac{3n}{2}} \int \cdots \int \prod_{m=1}^{n} d^3x^{(m)} e^{NF_1} \left| e^{iNF_2} \right| \\
&= \lim_{n\to\infty} \frac{2^N N^2}{(2\pi)^4} \int ds \int d^3r \left(\frac{N}{2\pi n(a^2+k^2)} \right)^{\frac{3n}{2}} \int \cdots \int \prod_{m=1}^{n} d^3x^{(m)} e^{NF_1}.
\end{aligned} \tag{8.17}$$

The remaining integral in the bound can be solved by Laplace's method in the $N \to \infty$ limit to give

$$\Omega_\infty(\epsilon, \underline{m}) \leq C e^{N(\ln 2 + F_0)}, \tag{8.18}$$

where C is a prefactor which is sub-exponential in N and F_0 is the absolute minimum of the real part F_1 of F. Substituting this into the entropy and considering the limit $N \to \infty$ we have the bound

$$s_\infty \leq \ln(2) + F_0. \tag{8.19}$$

8.2.4 (c) Lower bound for the entropy

In the canonical calculation reported in [34], the lower bound for the free energy is obtained by using Bogoliubov's inequality [41] which states

$$f[H_0 + H_1] \leq f[H_0] + \langle H_1 \rangle_{H_0}. \tag{8.20}$$

Here $f[A] = -\frac{1}{\beta} \ln tre^{-\beta A}$ and $\langle A \rangle_B = \frac{TrAe^{-\beta B}}{Tre^{-\beta B}}$. This inequality is proved by introducing a real parameter, λ, in the exponent, A, of f and proving that f is concave in terms of this parameter. When we then set $\lambda = 1$, (8.20) is obtained.

This proof is only valid if the exponent in f is real. In the microcanonical ensemble the function F, analogous to G in the canonical ensemble, is not necessarily real so that this inequality is not applicable in the microcanonical ensemble.

As a concluding remark on this method, we notice that there are two problems when trying to implement this method. Firstly we are not able to prove that a certain stationary point yields the absolute maximum, F_0 of the real part the function F. Secondly we are not able to show that there exists a lower bound for the entropy $s_\infty \geq \ln(2) + F_0$. Therefore we were not able to apply the method implemented in [34] in the microcanonical case.

8.3 Solution for the entropy

We now resort back to the method of steepest decent. We want to deform the contour of integration of the complex integrals in (7.21) so that the function F, in (7.21), has a constant imaginary part, F_2, and then look for the maximum of the real part on that contour. This corresponds to simultaneously solving the following equations for s ,$\underline{r}$ and $\{\underline{x}^{(m)}\}$

$$\frac{\partial F}{\partial s} = \epsilon + \frac{1}{2ns^2} \sum_{u=1}^{n} \underline{x}^{(u)} \cdot \underline{x}^{(u)} = 0, \tag{8.21}$$

$$\frac{\partial F}{\partial r_\alpha} = m_\alpha + \frac{\tanh a}{a} \left(r_\alpha - \frac{\sqrt{\lambda_\alpha}}{n} \sum_{u=1}^{n} x_\alpha^{(u)} \right) = 0, \tag{8.22}$$

$$\frac{\partial F}{\partial x_\alpha^{(u)}} = -\frac{x_\alpha^{(u)}}{ns} - \frac{\tanh a}{a} \left(r_\alpha - \frac{\sqrt{\lambda_\alpha}}{n} \sum_{u=1}^{n} x_\alpha^{(u)} \right) \frac{\sqrt{\lambda_\alpha}}{n} = 0, \tag{8.23}$$

for $\alpha = (1, 2, 3)$. This set of solutions corresponds to the correct result if the real part, F_1, does indeed have a maximum on the contour where the imaginary parts are constant. An interesting

observation is that for some initial values used in a numerical routine in *Mathematica*, no real solutions were found for the stationary point equations. This indicates that the stationary point equations may not have real solutions, in contrast to the cases reported in [34] [39]. The relevant question to ask is if this is unique to the microcanonical ensemble, since the calculations reported in the references are both in the canonical ensemble.

Notice that setting (8.22) into (8.23) and doing some straightforward algebra leads to

$$x_\alpha^{(u)} - m_\alpha s\sqrt{\lambda_\alpha} = 0, \tag{8.24}$$

which in turn implies that $x_\alpha^{(u)} = m_\alpha s\sqrt{\lambda_\alpha} = x_\alpha \; \forall \; u \in \{1, \cdots, n\}$. This is the result obtained for the stationary points in the canonical calculation in [34], which we tried to prove in section 8.2.2. Using this in equations (8.21) - (8.23) leads to

$$\begin{aligned} 0 &= 2\epsilon s^2 + \underline{x} \cdot \underline{x}, && (8.25)\\ 0 &= am_\alpha + \left(r_\alpha - \sqrt{\lambda_\alpha} x_\alpha\right) \tanh a, && (8.26)\\ 0 &= x_\alpha - m_\alpha s\sqrt{\lambda_\alpha}, && (8.27) \end{aligned}$$

We can use this set of equations to simultaneously solve for the variables s, $\underline{r}$ and $\underline{x}$ in terms of ϵ and m. The calculation is explicitly shown in Appendix A. The resulting expression for F is then

$$F(\epsilon, \underline{m}) = -|\underline{m}| \; \text{arctanh}|\underline{m}| - \frac{1}{2}\ln(1 - |\underline{m}|^2), \tag{8.28}$$

with

$$|\underline{m}| = \sqrt{m_1^2 + m_2^2 + m_3^2}. \tag{8.29}$$

Substituting this value of F into the expression for the density of states (7.21), we get

$$\Omega_N(\epsilon, \underline{m}) \approx C2^N \exp\left[-|\underline{m}| \; \text{arctanh}|\underline{m}| - \frac{1}{2}\ln(1 - |\underline{m}|^2)\right]. \tag{8.30}$$

Here C is some prefactor which is sub-exponential in N. This prefactor can be neglected because we want to use the density of states in the expression for the entropy,

$$s(\epsilon, \underline{m}) = \lim_{N\to\infty} \frac{1}{N} \ln \Omega_N(\epsilon, \underline{m}), \tag{8.31}$$

where it is clear that terms that are sub-exponential in N will vanish in the $N \to \infty$ limit. Finally we have

$$s(\epsilon, \underline{m}) = \ln(2) - |\underline{m}| \operatorname{arctanh}|\underline{m}| - \frac{1}{2}\ln(1 - |\underline{m}|^2). \tag{8.32}$$

Although this might seem surprising, since the value of the entropy only depends on the size of the magnetisation, the energy is intrinsically dependent on the magnetisation through

$$\epsilon = -\frac{1}{2}\sum_{i=1}^{3} \lambda_i m_i^2. \tag{8.33}$$

The expression for the entropy is a function which is dependent on three variables, m_1, m_2 and m_3. Depending on what we want to observe it might be useful to use expression (8.33) for the energy to rewrite

$$m_1 = \sqrt{-\frac{2\epsilon + \lambda_2 m_2^2 + \lambda_3 m_3^2}{\lambda_1}}, \tag{8.34}$$

so that

$$|\underline{m}| = \sqrt{\frac{1}{\lambda_1}[(\lambda_1 - \lambda_2)m_2^2 + (\lambda_1 - \lambda_3)m_3^2 - 2\epsilon]}. \tag{8.35}$$

To test if this result for the entropy is correct we compare this result with the calculation reported in [26] for the same model but with magnetic field only in the z-direction, $\underline{h} = (0, 0, h)$. Substituting this into the above expression for $\underline{m}$ in terms of ϵ we get

$$|\underline{m}| = \sqrt{\frac{1}{\lambda_{12}}[(\lambda_{12} - \lambda_3)m^2 - 2\epsilon]}. \tag{8.36}$$

In this expression λ_{12} is $\max\{\lambda_1, \lambda_2\}$. This arises from the fact that we can rewrite m_1 or m_2 in terms of the energy (8.33), but the correct entropy corresponds to the substitution that maximizes the entropy and therefore minimizes $\underline{m}$. This expression is identical to the result obtained in [26].

CHAPTER 9
Results

Now that we have an explicit expression for the entropy we want to see under which circumstances the entropy is a non-concave function in terms of the intensive system parameters. The solution we have for the entropy is as a function of internal energy, ϵ, and magnetisation, m. The energy here is not the total energy corresponding to the full Hamiltonian, but only the internal energy corresponding to the H_0 part consisting of the $\sigma_i\sigma_j$ interactions in (6.1). This entropy, as discussed in chapter 7, contains all the information of the external magnetic field dependence of the system. We will use this fact in section 9.3 to make a change of variables from internal energy, ϵ, and magnetisation, m, to total energy, u, and external magnetic field, h. Before we do this, we want to see under which circumstances, if any, the entropy is a non-concave function in terms of internal energy, ϵ, or magnetisation, m. Let us consider the case when we use (8.33) to make the substitution

$$m_3 = \sqrt{-\frac{2\epsilon + \lambda_1 m_1^2 + \lambda_2 m_2^2}{\lambda_3}}, \tag{9.1}$$

so that

$$m_1^2 + m_2^2 + m_3^2 = \frac{1}{\lambda_3}[(\lambda_3 - \lambda_1)m_1^2 + (\lambda_3 - \lambda_2)m_2^2 - 2\epsilon]. \tag{9.2}$$

This we can use in the entropy (8.32) to get it in the following form

$$s(\epsilon, m_1, m_2) = \ln(2) - \alpha \operatorname{arctanh}(\alpha) - \frac{1}{2}\ln(1-\alpha^2), \tag{9.3}$$

where

$$\alpha = \alpha(\epsilon, m_1, m_2) = \sqrt{\frac{1}{\lambda_3}[(\lambda_3 - \lambda_1)m_1^2 + (\lambda_3 - \lambda_2)m_2^2 - 2\epsilon]}. \tag{9.4}$$

9.1 Convexity of $s(\epsilon, m_1, m_2)$

We want to discuss the convexity properties of $s(\epsilon, m_1, m_2)$. From previous results [26] we know that the entropy will be non-concave in terms of m_i if $\lambda_i > \lambda_3$ for $m_j = 0$. Since we are limited graphically to representing the function in terms of two variables let us consider $s(\epsilon, m_i)_{m_j}$, meaning that we consider the function $s(\epsilon, m_i)$ at a given magnetisation m_j, where $i, j \in \{1, 2\}$, $i \neq j$. In figure 9.1 plots of the entropy in terms of ϵ and m_i are shown for different values of m_j. We observe that the entropy is indeed non-concave in terms of m_i, at a fixed

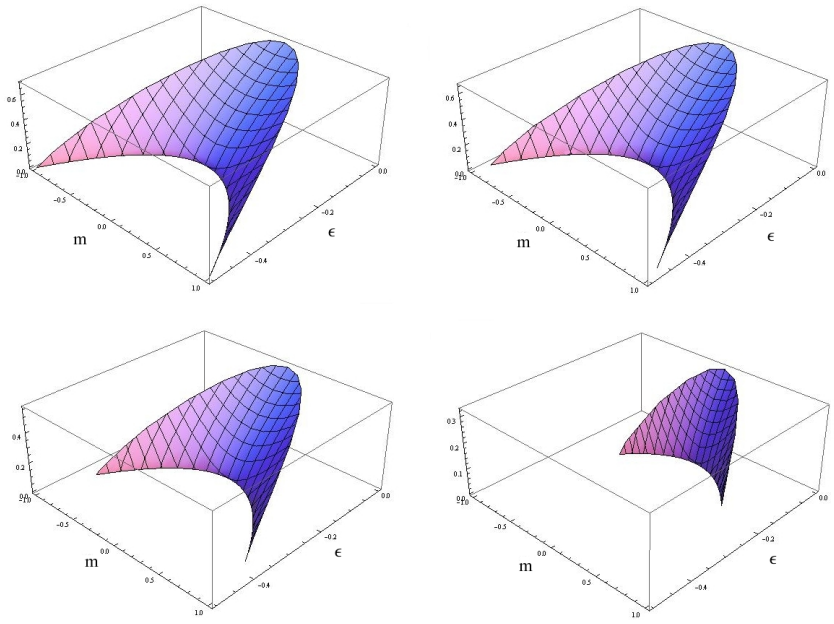

Figure 9.1: Non-concave entropies for $(\lambda_1, \lambda_3) = (1, 1/2)$ with $m_j = 0, 1/4, 1/2, 4/5$ respectively. Note that as m_j increases the function remains non-concave but the allowed domain decreases

value of the internal energy, and remains non-concave with only the allowed domain changing as m_j is increased.

In figure 9.2 the same effect is observed for a concave entropy $\lambda_3 > \lambda_1$. We can conclude at this point that the convexity properties of $s(\epsilon, m_i, m_j)$ in terms of m_i are only dependent on the sign of $(\lambda_3 - \lambda_i)$ whereas λ_j and m_j only influence the allowed domain. Although the discussion here is limited to the convexity properties in terms of m_i the exact same argument holds for the convexity properties in terms of m_j so that we only need to determine the sign of $(\lambda_3 - \lambda_j)$.

It is clear from the plots that the entropy is concave in terms of energy at fixed values of the magnetisation for all combinations of the coupling constants. The entropy is non-concave in terms of magnetisation at fixed energies for certain combinations of the coupling constants, therefore the microcanonical and canonical ensembles are non-equivalent in terms of magnetisation and external magnetic field for these combinations of the coupling constants at fixed energy, since the entropy is non-concave.

9.2 Magnetic susceptibility

Since we now know that the entropy can be a non-concave function in terms of the magnetisation, m, we would like to see if the magnetic susceptibility can be negative and under what

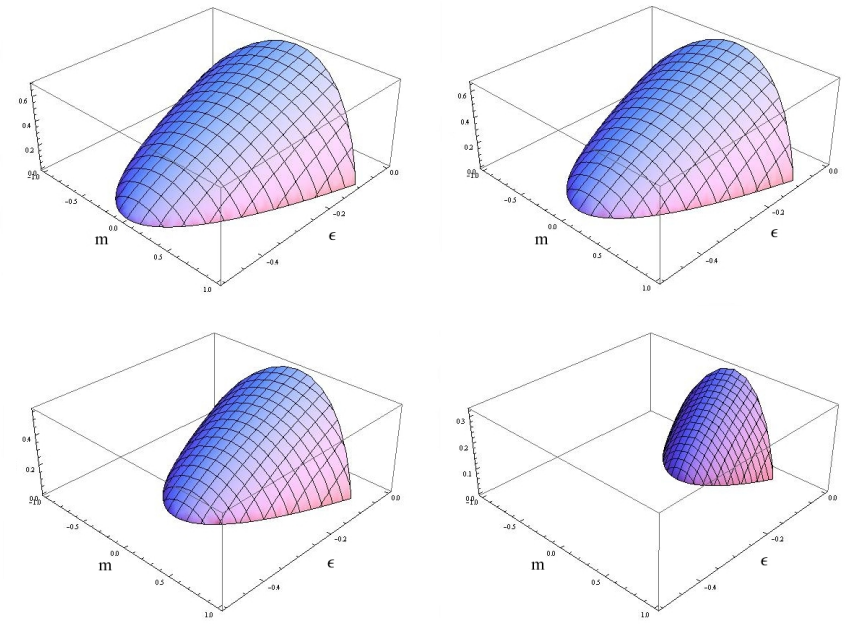

Figure 9.2: Concave entropies for $(\lambda_1, \lambda_3) = (1/5, 1)$ with $m_j = 0, 1/4, 1/2, 8/10$ respectively. Note that as m_j increases the function remains concave but the allowed domain decreases

circumstances this will be the case. We remind the reader that the magnetic susceptibility does not necessarily only depend on the curvature of the entropy in terms of magnetisation, so that we cannot conclude that the magnetic susceptibility is negative even though the entropy is a non-concave function in terms of m. The magnetic susceptibility, introduced in (4.9), is given by

$$\chi(\epsilon, m) = \left(\frac{\partial s}{\partial \epsilon}\right)^2 \left(\frac{\partial^2 s}{\partial m \partial \epsilon}\frac{\partial s}{\partial m} - \frac{\partial s}{\partial \epsilon}\frac{\partial^2 s}{\partial m^2}\right)^{-1}. \tag{9.5}$$

Since we have the entropy as a function of energy and magnetisation in two directions $s(\epsilon, m_i, m_j)$ where $i,j \in \{1, 2, 3\}$ with $i \neq j$, we can get the directional magnetic susceptibility

$$\chi(\epsilon, m_i) = \left(\frac{\partial s}{\partial \epsilon}\right)^2 \left(\frac{\partial^2 s}{\partial m_i \partial \epsilon}\frac{\partial s}{\partial m_i} - \frac{\partial s}{\partial \epsilon}\frac{\partial^2 s}{\partial m_i^2}\right)^{-1}. \tag{9.6}$$

Then substituting the expression for the entropy $s(\epsilon, m_i, m_j)$ in (9.3) into this expression yields

$$\chi(\epsilon, m_i) = \frac{1}{\lambda_{j,k} - \lambda_i}. \tag{9.7}$$

where $\lambda_{j,k}$ is $\max\{\lambda_j, \lambda_k\}$. This expression is remarkably simple and it is surprising that the

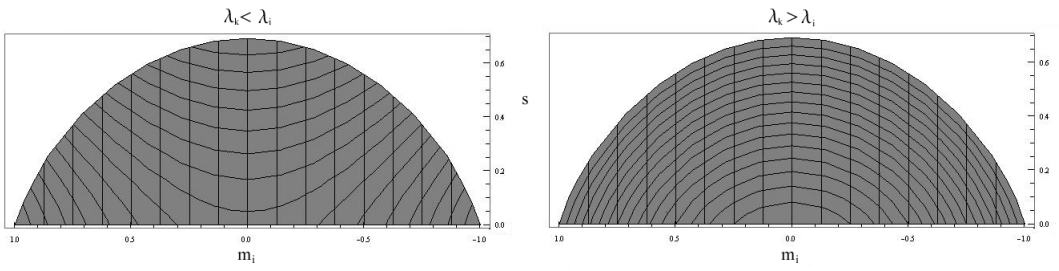

Figure 9.3: The entropy as a function of magnetisation in the i-direction, the different lines correspond to different energies, the bottom lines corresponds to an energy $\epsilon = -0.5$ and the top line corresponds to $\epsilon = 0$. The entropy is strictly concave when $\lambda_k > \lambda_i$ and the magnetic susceptibility is positive. When $\lambda_k < \lambda_i$ the entropy is strictly non-concave and the magnetic susceptibility is negative.

magnetic susceptibility is only dependent on the coupling constants. Note that the magnetic susceptibility is negative whenever $\lambda_i > \lambda_{j,k}$, and this coincides with the entropy being non-concave. In figure 9.3 the entropy is shown in terms of the magnetisation for different energies. This differs from other published results, for instance [21], where there are values of m for which the entropy is convex for a fixed energy but for stronger magnetisation the entropy is concave. Therefore magnetic susceptibility has a clear energy and magnetisation dependence in these cases.

9.3 Changing variables

As mentioned in section 5.2, the magnetisation is not a conserved quantity under time evolution in the model (6.1) considered, so that it is not a good quantity to distinguish equilibrium states since it will not be constant. The external magnetic field is a quantity that is easily controllable and is a better candidate for describing equilibrium states of a long-range spin model. Therefore in order to compare the behaviour of an experimental system with our model we need to transform the variables internal energy, ϵ, and magnetisation, m, to mean energy, u, and external magnetic field, h. We can use the expression for the total energy of the N particle system, given by

$$u = \epsilon - \underline{h} \cdot \underline{m}, \tag{9.8}$$

to get the entropy in the suitable form. The entropy in terms of magnetisation was computed (8.32) as

$$s(m_1, m_2, m_3) = \ln(2) - \alpha \operatorname{arctanh}(\alpha) - \frac{1}{2}\ln(1 - \alpha^2), \tag{9.9}$$

where

$$\alpha = \alpha(m_1, m_2, m_3) = \sqrt{m_1^2 + m_2^2 + m_3^2}. \tag{9.10}$$

Now we want to eliminate one of the magnetisation variables in (9.10) to introduce the mean energy, u. We can do this by using (9.8) together with (8.33) to get the quadratic equation

$$\sum_{i=1}^{3} \lambda_i m_i^2 + 2\sum_{j=1}^{3} h_j m_j + 2u = 0. \tag{9.11}$$

The solution of one of the magnetisation variables is then given by

$$m_i(u, m_j, m_k) = -\frac{h_i}{\lambda_i} \pm \sqrt{\left(\frac{h_i}{\lambda_i}\right)^2 - (\lambda_j m_j^2 + \lambda_k m_k^2 + 2h_j m_j + 2h_k m_k + 2u)}, \tag{9.12}$$

for i,j,$k \in \{1, 2, 3\}$, $i \neq j \neq$ k. We can use this expression for the magnetisation (9.12), to introduce a new $\tilde{s}$,

$$\tilde{s}_{\underline{h}}(u, m_j, m_k) = \ln(2) - \tilde{\alpha}_{\underline{h}} \operatorname{arctanh}(\tilde{\alpha}_{\underline{h}}) - \frac{1}{2}\ln(1 - \tilde{\alpha}_{\underline{h}}^2), \tag{9.13}$$

where

$$\tilde{\alpha}_{\underline{h}} = \tilde{\alpha}_{\underline{h}}(m_i(u, m_j, m_k), m_j, m_k) = \sqrt{m_i^2(u, m_j, m_k) + m_j^2 + m_k^2}. \tag{9.14}$$

Here $m_i((u, m_j, m_k), m_j, m_k)$ is the solution to the quadratic equation (9.11) given by (9.12). To have the entropy only in terms of total energy, u, we need to maximize the entropy, $\tilde{s}$ in terms of m_j and m_k,

$$\tilde{s}_{\underline{h}}(u) = \max_{m_j, m_k} \tilde{s}_{\underline{h}}(u, m_j, m_k), \tag{9.15}$$

for j,$k \in \{1, 2, 3\}$, $j \neq k$. This corresponds to finding the values of m_j and m_k that satisfy

$$\frac{\partial \tilde{s}}{\partial m_j} = \frac{\operatorname{arctanh}(\tilde{\alpha}_{\underline{h}})}{\tilde{\alpha}_{\underline{h}}} \frac{\partial(\tilde{\alpha}_{\underline{h}}^2)}{\partial m_j} = 0 \tag{9.16}$$

$$\frac{\partial \tilde{s}}{\partial m_k} = \frac{\operatorname{arctanh}(\tilde{\alpha}_{\underline{h}})}{\tilde{\alpha}_{\underline{h}}} \frac{\partial(\tilde{\alpha}_{\underline{h}}^2)}{\partial m_k} = 0 \tag{9.17}$$

These expressions can be simplified since $\frac{\operatorname{arctanh}(\tilde{\alpha}_{\underline{h}})}{\tilde{\alpha}_{\underline{h}}} \neq 0$ so we are only left with solving m_j and m_k for the equations

$$\frac{\partial(\tilde{\alpha}_{\underline{h}}^2)}{\partial m_j} = 0 \tag{9.18}$$

$$\frac{\partial(\tilde{\alpha}_{\underline{h}}^2)}{\partial m_k} = 0 \tag{9.19}$$

This might seem like an easy task, but the general solution to the problem is not a closed form expression. We will look at a few simplified examples.

9.3.1 Isotropic Heisenberg model

The first example we will consider is the isotropic Heisenberg model where $\lambda_1 = \lambda_2 = \lambda_3 = 1$. The solutions for this model for equations (9.12),(9.16) and (9.17) for $i \in \{1, 2, 3\}$ are

$$m_i = -h_i(1 \pm \sqrt{1 - \frac{u}{h^2}}), \tag{9.20}$$

where $h = |\underline{h}|$. Hence

$$\tilde{s}_{\underline{h}}(u) = \ln(2) - \tilde{\alpha}_{\underline{h}} \operatorname{arctanh}(\tilde{\alpha}_{\underline{h}}) - \frac{1}{2}\ln(1 - \tilde{\alpha}_{\underline{h}}^2), \tag{9.21}$$

where

$$\tilde{\alpha}_{\underline{h}} = \sqrt{h^2\left(1 - \operatorname{sgn}(h)\sqrt{1 - \frac{u}{h^2}}\right)^2}. \tag{9.22}$$

Notice here that the direction of the magnetic field does not matter since the coupling is equal in all directions. Therefore there is no competition between the coupling term and magnetic field term in the Hamiltonian (6.1). To have this competition, we need a difference in the strongest coupling direction and magnetic field, so that the coupling between particles in one direction dominates at certain energies and the coupling between the magnetic field and spin in a different direction dominates at different energies. In figure 9.4 the plot of the entropy as a function of the external magnetic field strength and total energy is shown. Note that there is a field-driven first order phase transition line (non-continuous first derivative) at $h = 0$ for total energy from -0.5 to 0. This phase transition is between the spins aligned in the positive z-direction or the negative z-direction.

9.3.2 Ising model

The next case we will study is the Curie-Weiss Ising model where $\lambda_1 = \lambda_2 = 0$ and $\lambda_3 = 1$. First we consider the transverse field Ising model where the magnetic field is in the xy-plane, with θ the angle of the magnetic field between the x- and y-axis, while the coupling is in the z-direction. In this case there are two sets of solutions for the variables corresponding to different domains in the u-h plane. If $u < -h^2$ then

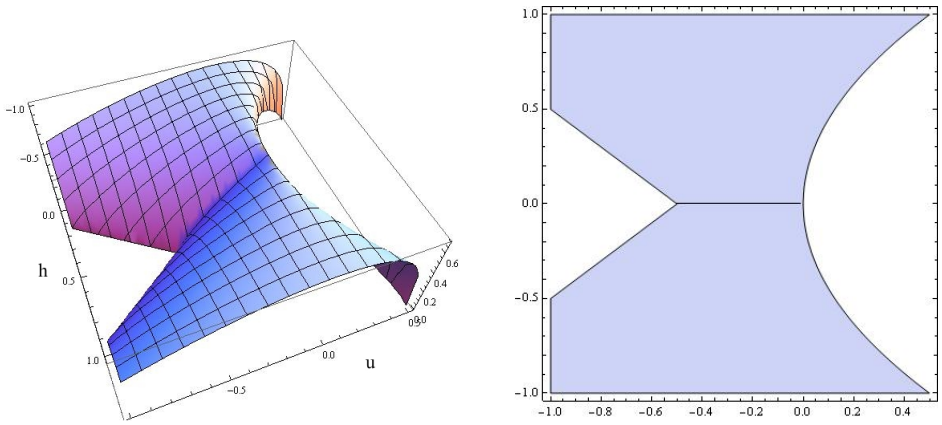

Figure 9.4: The entropy as a function of magnetic field strength, h, and total energy, u, for the isotropic Heisenberg model. Note that there is a first order phase transition at the line $h = 0$ for energies between -0.5 and 0. The system here only has a ferromagnetic phase since there is no competition between the coupling and magnetic field.

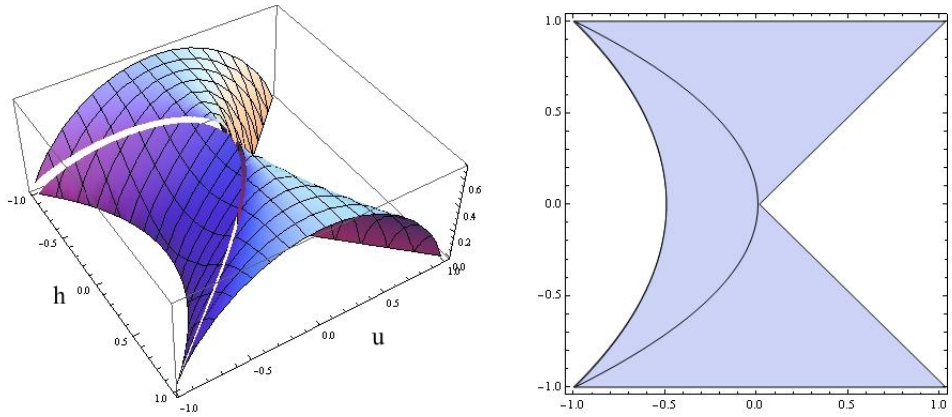

Figure 9.5: The entropy as a function of magnetic field strength, h, and total energy, u, for the transverse field Ising model. Note that there is a second order phase transition at the line $u = -h^2$ between a ferromagnetic and paramagnetic phase.

$$m_1 = h_1 = h\cos\theta, \tag{9.23}$$

$$m_2 = h_2 = h\sin\theta, \tag{9.24}$$

$$m_3 = \sqrt{-2h^2 - 2u}, \tag{9.25}$$

so that

$$\tilde{\alpha}_{\underline{h}} = \sqrt{-h^2 - 2u} \tag{9.26}$$

If $u > -h^2$ then

$$m_1 = 0, \tag{9.27}$$

$$m_2 = 0, \tag{9.28}$$

$$m_3 = -\frac{u}{h}, \tag{9.29}$$

so that

$$\tilde{\alpha}_{\underline{h}} = \sqrt{\frac{u^2}{h^2}} \tag{9.30}$$

Figure 9.5 shows a plot of the entropy function. Notice, from the definition 3 in section 4.6, that there is a second order (continuous) phase transition at the line $u = -h^2$, since here two neighbouring phases (different solutions for the entropy function) become indistinguishable. For the states that are to the left of the phase transition line the system is in a ferromagnetic phase and the coupling between the spins are dominant over the influence of the magnetic field. For a constant, non-zero magnetic field if the energy is increased the magnetic field term dominates and there is a second order phase transition to a paramagnetic phase.

Notice that for the Ising model if we consider a magnetic field in the z-direction (same direction as the coupling) the entropy will be equivalent to the entropy of the isotropic Heisenberg model so this will not be an interesting case to look at. We are instead interested in looking at a magnetic field that is not pointing along any of the axes, so we expect some behaviour in between the Heisenberg and the transverse field Ising model. First we need to examine the influence of the coupling constants.

9.3.3 Varying coupling constants with constant field direction

Consider a system with a magnetic field in the x-direction $\underline{h} = |h|\,\hat{i}$, where $\hat{i}$ is the unit vector in the x-direction and coupling only in the xy-plane ($\lambda_3 = 0$) with the constraint $\lambda_1 + \lambda_2 = 1$. This configuration is depicted in figure 9.6. In figure 9.7 the plots of the entropy function are shown with the coupling constants λ_1 and λ_2 being varied. When the strongest coupling is in the direction of the magnetic field a discontinuous first derivative at $h = 0$ appears so that the behaviour of the system is the same as for the isotropic Heisenberg model. When the strongest coupling is not in the direction of the magnetic field, two possible solutions for the entropy appear which indicate that a second order phase transition occurs between a paramagnetic phase and a ferromagnetic phase, as with the transverse field Ising model. When the strongest coupling is only slightly larger than the coupling in the direction of the magnetic field the domain of the solution which corresponds to the ferromagnetic phase

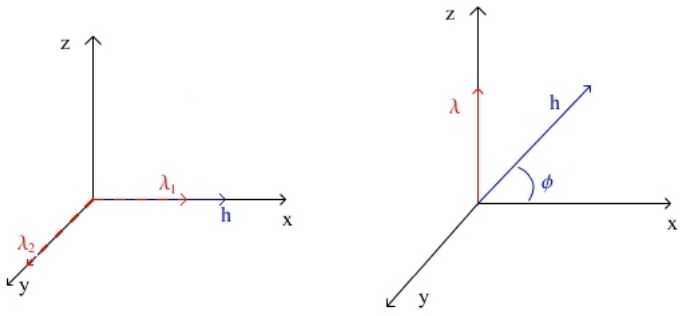

Figure 9.6: Graphic illustration of the two special cases we consider. The first is a constant magnetic field but with the values of the coupling constants changing in the x- and y-directions. The second case has constant coupling and the direction of the magnetic field changing between the x- and the z-axis.

is small (consider figure 9.7).

An important point arises when we discuss the properties of the phase transitions of these models which can be observed in figure 9.7. Only the direction of the strongest coupling is necessary to describe the existence and order of the phase transition of the system for an external magnetic field fixed to one of the axis directions, as seen in figure 9.7. This means that the existence and order of phase transitions for a system with a magnetic field fixed to one direction can be determined by considering either the transverse field- or longitudinal field Ising model.

9.3.4 Ising model with varying field direction

From the previous section we see that we only need to consider the strongest coupling when we want to determine the existence and order of phase transitions of the system. We can therefore set the coupling in the other directions to zero. We now want to see what the influence of the direction of the magnetic field is on the phase transition properties of the system. So let us consider the Curie-Weiss Ising model again ($\lambda_1 = \lambda_2 = 0$, $\lambda_3 = 1$), with a magnetic field $\underline{h} = |h| \cos\phi \hat{i} + |h| \sin\phi \hat{k}$, where $\hat{i}$ and $\hat{k}$ are unit vectors in the x- and z-directions respectively and ϕ is the azimuthal angle between the x-axis and the magnetic field. This configuration is represented in figure 9.6. In Appendix B the explicit solutions are given for this special case. In figure 9.8 numerous plots of the entropy function are given for different values of the angle ϕ.

Here it is noticeable that the first derivative at $h = 0$ immediately becomes discontinuous when the field is not orientated along the x-axis. This is intuitive in the sense that when

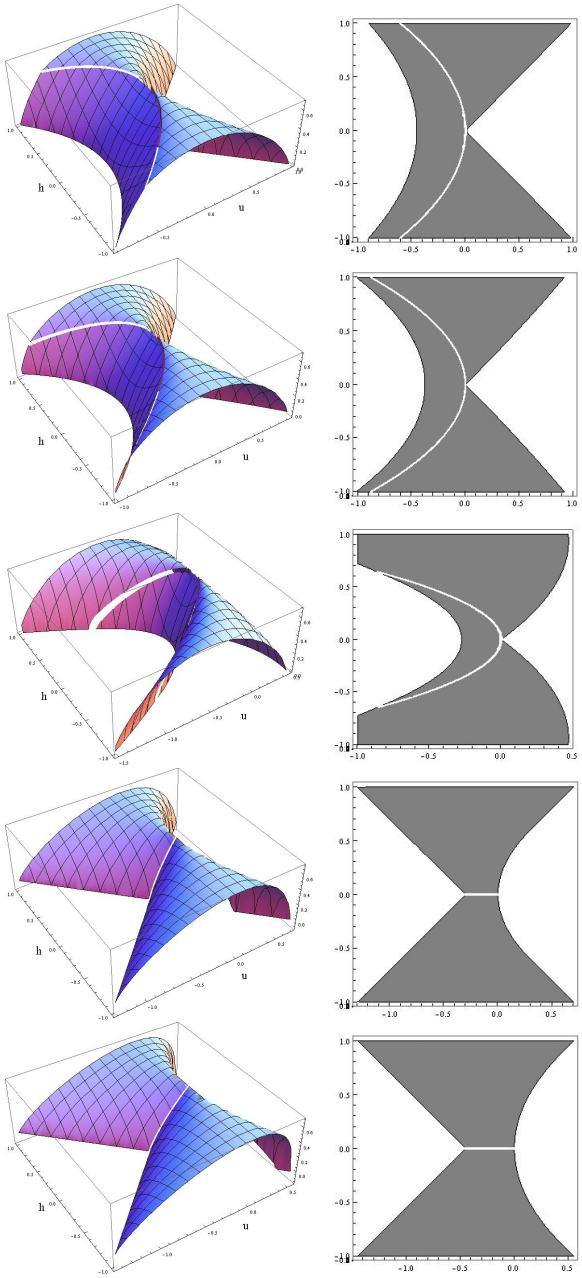

Figure 9.7: The entropy as a function of magnetic field strength, h, and total energy, u, for the special case $\underline{h} = (h, 0, 0)$ and $(\lambda_1, \lambda_2) = (1/10, 9/10)$, $(1/4, 3/4)$, $(9/20, 11/20)$, $(6/10, 4/10)$ and $(9/10, 1/10)$ respectively. Here we see that if $\lambda_1 < \lambda_2$ only the second order phase transition line at $u = \frac{h^2(\lambda_1 - 4\lambda_2)}{2(\lambda_1 - 2\lambda_2)^2}$ is present and if $\lambda_1 > \lambda_2$ only the first order phase transition at $h = 0$ is present.

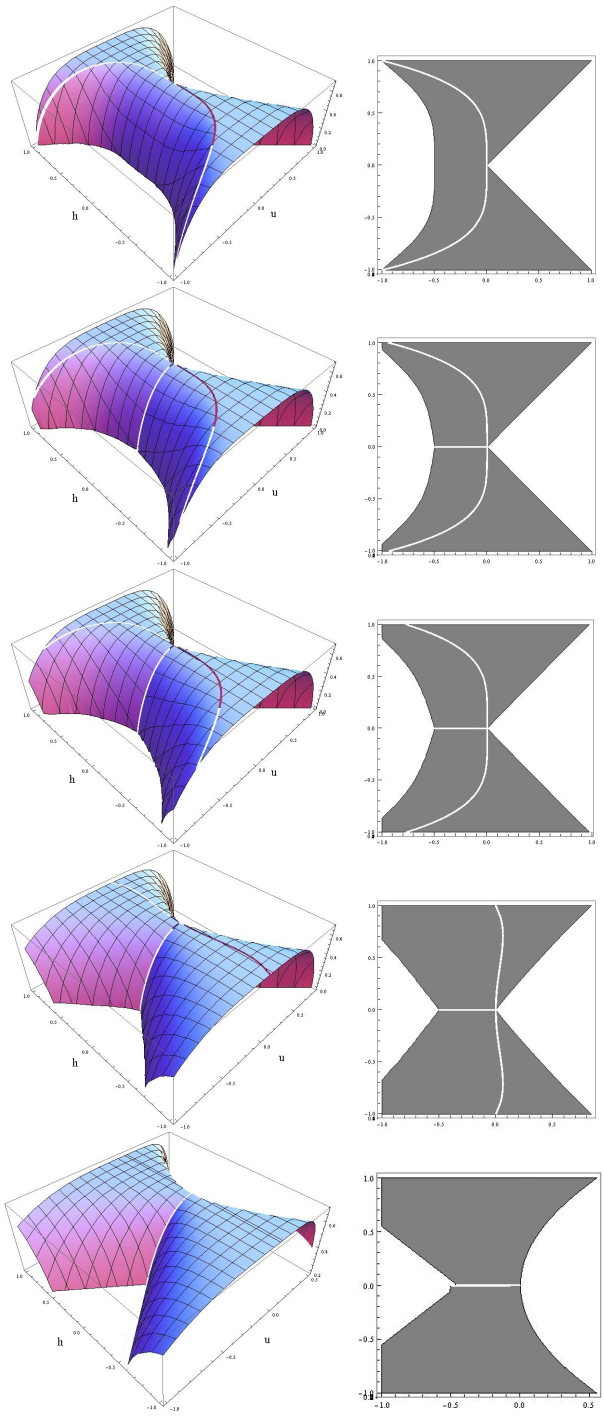

Figure 9.8: The entropy as a function of magnetic field strength, h, and total energy, u, for the special case $(\lambda_1, \lambda_2, \lambda_3) = (0, 0, 1)$ and $\underline{h} = (h\cos\phi, 0, h\sin\phi)$ where $\phi = 0$, $\frac{\pi}{20}$, $\frac{\pi}{10}$, $\frac{\pi}{4}$ and $\frac{\pi}{2}$ respectively. Note here that for the two boundary cases when the field is in a transverse ($\phi = 0$) or longitudinal ($\phi = \pi/2$) direction only one phase transition line is present. In the transverse case only the second order and for the longitudinal only the first order. For the cases in between both phase transition lines are present: the first order transition line at $h = 0$ and the second order transition line at $u = -(h\cos\theta)^4 + \frac{1}{2}(h\sin\theta)^2$. When the angle between the magnetic field and the coupling decreases the magnetic field has to increase to drive the system to a paramagnetic phase.

the system is at a ferromagnetic phase (at low energy) the coupling term dominates the entropy. Since the magnetic field is in a transverse direction, the system at these energies will equilibrate in the coupling direction and the sign of the direction is only determined by the initial conditions. In the case when the magnetic field is pointing only slightly in the positive or negative direction of the coupling, the spins will align in this particular direction, since the magnetic field will give this direction a slight dominance over the other. Therefore the first order phase transition line appears.

The second order phase transition, as with the transverse field Ising model, is present (although not always visible in the plots) for all the graphs except when $\phi = \pi/2$. This results from the multiple solutions for $\underline{m}$ depending on the sign of the square root term as described in Appendix B. The smaller the angle between the magnetic field and the coupling direction, the stronger the magnetic field needs to be to drive the system to a paramagnetic phase. When the field is pointing in the direction of the coupling then only the ferromagnetic phase exists since there is no competition between the coupling and the magnetic field.

Notice in the fourth plot of figure 9.8 that the second order phase transition line is not confined to only the domain where the entropy is an increasing or decreasing function of energy, u, so that the phase transition line can be at positive and negative temperatures (see definition in section 9.4) depending on the strength of the magnetic field. This will be discussed in section 9.4. This implies, amongst other things, that the phase transition properties of the systems where the magnetic field is not fixed to one axial direction cannot be described by the transverse- or longitudinal field Ising model as was the case in section 9.3.3.

9.3.5 Contradicting results

After the first submission of this thesis, it was noticed that sections 9.3.3 and 9.3.4 give contradicting results. One should be able to construct rotated Pauli-operators so that the two scenarios have identical Hamiltonians. Due to rotational invariance, the only quantity that matters should be the angle between the field vector and the coupling vector. Since in this section, the field goes from being aligned with the coupling to perpendicular to the coupling in both cases, the quantitative differences between the two scenarios are not reasonable. This issue will be resolved in a forthcoming publication.

9.4 Temperature at the second order phase transition line

In the canonical ensemble the temperature of the system is generally assumed to be positive, this is because the heat bath a system is coupled to is generally assumed to have positive temperatures in order to mimic physical situations. In the microcanonical ensemble the temperature, which is defined as

$$\frac{\partial s}{\partial u} = \frac{1}{T}, \tag{9.31}$$

can be negative. Therefore if we have a phase transition at negative temperature in the microcanonical ensemble, this phase transition will not be represented in the canonical ensemble if we consider the above mentioned assumption.

Bearing this in mind, consider in figure 9.8 that the second order phase transition line appears to be in a region where the temperature is positive if the magnetic field is pointing predominantly in the direction of the coupling. As the angle, ϕ, between the magnetic field and coupling is increased, the phase transition line tends to move to a region where the slope of the entropy is negative (i.e negative temperature) when the strength of the magnetic field is small. To investigate this consider the plots in figure 9.9 for the entropy of the Ising model with field direction varying between 0 and $\pi/2$, alongside the value of the inverse temperature at the second order phase transition line. From the plots we see that the temperature at the phase transition line is positive when the magnetic field is in the direction of the coupling ($\phi = 0$) and negative when the magnetic field is in a transverse direction to the coupling ($\phi = \pi/2$) and for the cases in between the phase transition line is at positive and negative temperature. The phase transitions at negative temperatures are not represented in the canonical ensemble when adopting the usual convention of heat baths with only positive temperatures.

9.5 Concavity of $s_{\underline{h}}(u)$

A disappointing aspect of the entropy plots is the lack of a non-concave entropy in terms of the variable u when the magnetic field h is kept fixed. Since the magnetic field, h, is not a macrostate of the system, the non-concavity properties of the entropy in terms of h at a fixed u does not correspond to non-equivalence of ensembles. The presence of the equilibrium states that correspond to the non concave part of the entropy in terms of u would be the states that could be experimentally verified, by detecting negative specific heat with cold atoms in optical lattices. It would be an interesting follow-up to this thesis to try and find other models where this could be observed.

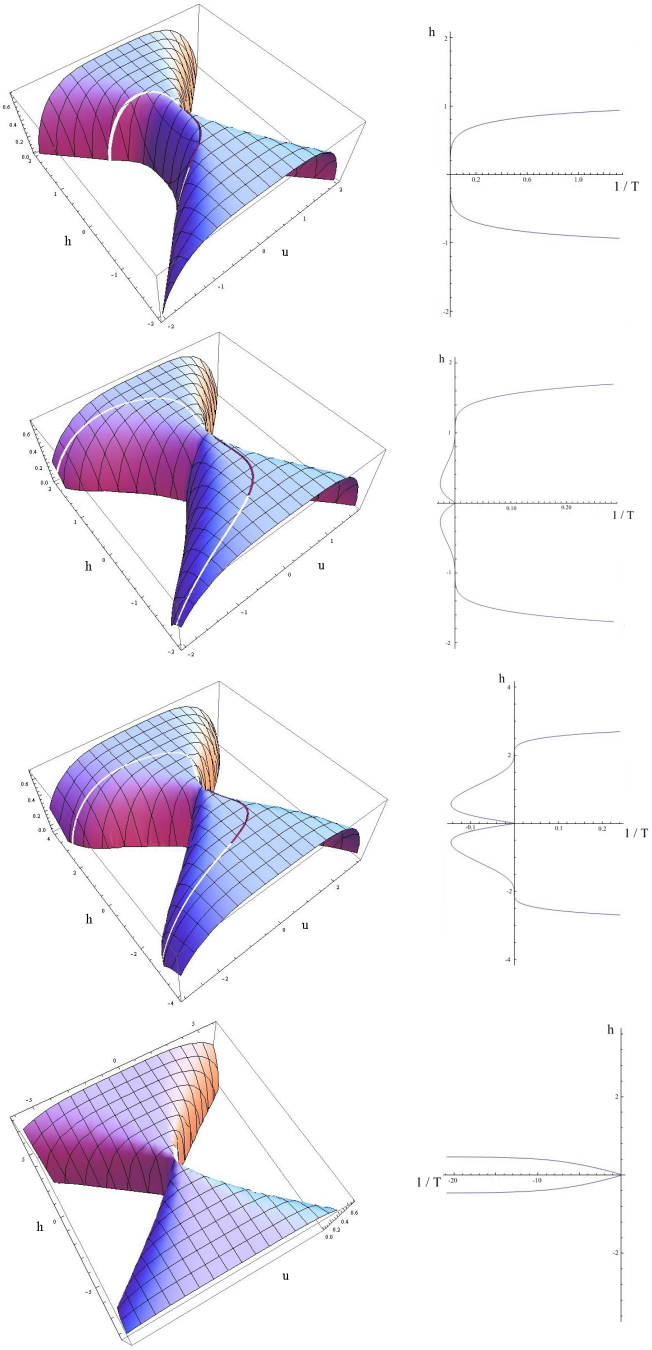

Figure 9.9: The entropy as a function of magnetic field strength, h, and total energy, u, for the special case $(\lambda_1, \lambda_2, \lambda_3) = (0, 0, 1)$ and $\underline{h} = (h\cos\phi, 0, h\sin\phi)$ for $\phi = 0.05$, 0.8, 1.0 and 1.4 radians respectively. Alongside these plots are the values of the inverse temperature $\beta = 1/T$ at the second order phase transition line, $u = -(h\cos\theta)^4 + \frac{1}{2}(h\sin\theta)^2$. Note that when the system approaches the longitudinal field Ising model, $\phi \to 0$, the phase transition line is only at positive temperature. The scenarios between the longitudinal ($\phi \to 0$) and transverse ($\phi \to \pi/2$) have phase transitions at positive and negative temperatures. When the angle ϕ approaches $\pi/2$ (transverse field) the second order phase transition line collapses to the point $(u, h) = (0, 0)$.

CHAPTER 10
Conclusions

The main goal of this thesis is to contribute to the understanding of long-range quantum spin systems, with an emphasis on the different properties these systems exhibit depending on which physical situation they are realised in. For long-range systems the physical setting in which the system is considered can be important, since the different statistical ensembles to which they correspond may be non-equivalent. In short-range interacting systems this is not the case since the statistical ensembles are generally equivalent [16].

It has been shown that the anisotropic quantum Heisenberg model can be engineered with cold atoms in optical lattices with algebraically decaying long-range interactions [27]. Since in optical lattice experiments, the energy and particle number are conserved to a good degree, the appropriate setting to consider the system in would be the microcanonical one. The results for this model with Curie-Weiss type interactions in the canonical setting had been reported in [5] and a simplified variation of this model with Curie-Weiss interactions had been calculated in the microcanonical setting in [26]. Although this model cannot be engineered with Curie-Weiss type interactions, previous results indicate that the Curie-Weiss type interactions mimic long-range interactions to a good degree [30] [31] and therefore we have sufficient reason to believe that irregularities present for systems with Curie-Weiss type interactions will also be present in systems with algebraically decaying long-range interactions.

Since we know that the anisotropic quantum Heisenberg model can be physically realised in a microcanonical setting and that the canonical results of this model are known, we had to calculate the microcanonical entropy in order to compare the results of the different ensembles. To do this we discussed a suggestion by Truong [9] to formulate a microcanonical density of states in terms of variables that correspond to non-commuting operators. We then formulated the density of states for the Curie-Weiss anisotropic quantum Heisenberg model by doing an inverse Laplace transform of the canonical partition function. To solve the resulting integral we used similar techniques applied in [34] to write the expression for the density of states in a manner which can be solved analytically by asymptotic means in the thermodynamic limit. The solution for the entropy, $s(\epsilon, \underline{m})$, was given in terms of internal energy, ϵ, and magnetisation, m, in the thermodynamic limit. From there we recovered the entropy in terms of total energy, u, and external magnetic field, h.

To investigate the properties of the long-range quantum spin model, the resulting expression for the entropy, $s(\epsilon, \underline{m})$, was discussed. We noted that the entropy, $s(\epsilon, \underline{m})$, is concave

in terms of internal energy, ϵ, for fixed magnetisation for all circumstances. The entropy is however non-concave in terms of magnetisation, m_i, where $i \in \{1, 2, 3\}$ if the coupling in the i^{th} direction is not the strongest for fixed internal energy, ϵ. In these circumstances the microcanonical, with fixed internal energy ϵ, and canonical ensembles will be non-equivalent. This means that the magnetisation macro states that are represented in the non-concave part of the entropy will not be represented by macro states of the same model prepared in the canonical setting. We also investigated the value of the magnetic susceptibility, which showed that the system has a magnetic susceptibility, χ_i, that will be negative when the coupling in the i^{th} direction is not the strongest and that the magnetic susceptibility is independent of internal energy and magnetisation. Since the magnetic susceptibility is always positive in the canonical setting, this feature cannot be realised in a canonical condensed matter setting.

In optical lattice experiments, the magnetisation is not a conserved quantity in general. Therefore the value of the magnetisation will not be a good quantity to distinguish between equilibrium states since it will fluctuate. To investigate a more applicable scenario, we changed the variables internal energy, ϵ, and magnetisation, m, to total energy, u, and external magnetic field, h. The external magnetic field is a quantity which can easily be controlled in cold atom experiments and is therefore a better candidate to distinguish between equilibrium states than the magnetisation. The different properties of the entropy in terms of external magnetic field and total energy, $s_{\underline{h}}(u)$, were discussed. We noted that we only need to know the direction of strongest coupling to determine the existence and order of phase transitions when we consider the magnetic field in some fixed direction. Furthermore we observed that the entropy is a strictly concave function of total energy, u, so that the the specific heat is always positive. We noticed however, that a second order phase transition line can be present at negative temperatures in the microcanonical ensemble.

From the results of this thesis, it is clear that in certain circumstances the canonical setting will not be able to describe the properties of quantum spin systems prepared in the microcanonical setting. The properties that are present in the microcanonical ensemble but not in the canonical ensemble for the model we considered include: all macro states present in the non-concave parts of the entropy, the negative values of the magnetic susceptibility and the phase transitions at negative temperatures. Therefore if we want to describe the properties of a system like cold atoms in optical lattices with long-range interactions, the predictions of canonical calculations will not be sufficient.

CHAPTER 11
Outlook

In this chapter we mention some interesting questions that arose during the course of the thesis, which we were not able to resolve. In chapter 4 we mentioned some possible experiments where long-range quantum spin systems can be engineered with cold atoms in optical lattices. Unfortunately in the dipole-dipole interactions that were needed for the long-range interactions, the magnetisation is not a conserved quantity. Since the result of our calculation for the Curie-Weiss anisotropic quantum Heisenberg model only yielded a non-concave entropy in terms of magnetisation, the proposed dipole-dipole interactions would not be able to experimentally verify non-equivalence of ensembles. We offer two suggestions, very different in nature, to circumvent this problem.

The first, and most simple proposition is the formulation of a long-range interacting quantum spin system in an optical lattice where the magnetisation is a conserved quantity. Although it is not clear if this is possible, it would definitely be the most simple solution to the problem. Something similar to this suggestion is mentioned in section 4.1.1, where we propose to map the spin system to a lattice gas system. Since the particle density, which is the equivalent to magnetisation, is well conserved this could also cure this problem.

The second suggestion is to use the same methods we used in chapter 7 and 8 to solve other similar models, where we might see an entropy that is non-concave in terms of energy. This seems like the most plausible solution and would certainly be beneficial in more regards than just the verification of non-equivalence of ensembles, since the number of these type of solutions are very scarce in the literature.

In chapter 7 we used the same strategy as implemented in [34] to obtain the density of states for the ferromagnetic model ($\lambda > 0$) in a form that is solvable by asymptotic evaluation. Tindemans and Capel showed in [42] that a routine similar to this can be done for the antiferromagnetic case ($\lambda < 0$). It would be worthwhile to try and implement this method for the model we discussed for the antiferromagnetic case.

In chapter 8 we hinted at the idea that the stationary point equations do not have any strictly real solutions. This is in contrast to the canonical ensemble where the applicable solutions to the stationary point equations are normally on the real line. It may be interesting to study if this case is unique to the microcanonical ensemble.

APPENDIX A
Solving the saddle-point equations

Here we want to use equations (8.25),(8.26) and (8.27) to simultaneously solve the variables s, $\underline{r}$ and $\underline{x}$ in terms of ϵ and m. Substituting these solutions in the function F in (7.22) will give the solution for the density of states in the $N \to \infty$ limit.

We want to solve the variables s, $\underline{r}$ and $\underline{x}$ in terms of ϵ and m by using

$$\begin{aligned} 0 &= 2\epsilon s^2 + \underline{x} \cdot \underline{x} && \text{(A.1)} \\ 0 &= am_\alpha + \left(r_\alpha - \sqrt{\lambda_\alpha} x_\alpha\right) \tanh a && \text{(A.2)} \\ 0 &= x_\alpha - m_\alpha s \sqrt{\lambda_\alpha} && \text{(A.3)} \end{aligned}$$

and then substituting this into

$$F(s, \underline{r}, \underline{x}) = \epsilon s + \underline{r} \cdot \underline{m} - \frac{1}{2s} \underline{x} \cdot \underline{x} + \ln[\cosh(a(\underline{x}, \underline{r}))], \tag{A.4}$$

with a now given by

$$a(\underline{x}, \underline{r}) = \sqrt{\sum_{i=1}^{3} (r_i - \sqrt{\lambda_i} x_i)^2} \tag{A.5}$$

Notice from (A.2) that

$$(r_i - \sqrt{\lambda_i} x_i)^2 = \left(\frac{a}{\tanh a}\right)^2 m_i^2 \tag{A.6}$$

Summing on both sides and taking the square root

$$\sqrt{\sum_{i=1}^{3} (r_i - \sqrt{\lambda_i} x_i)^2} = \left(\frac{a}{\tanh a}\right) \sqrt{\sum_{i=1}^{3} m_i^2} = \left(\frac{a}{\tanh a}\right) |\underline{m}| \tag{A.7}$$

Set this in (A.5) to yield

$$a = \left(\frac{a}{\tanh a}\right) |\underline{m}| \,, \tag{A.8}$$

so that

$$a = \tanh^{-1} |\underline{m}| \tag{A.9}$$

Now using this in (A.4) together with the identity $2 \ln \cosh x = -\ln(1 - \tanh^2 x)$ gives

$$F(s, \underline{r}, \underline{x}) = \epsilon s + \underline{r} \cdot \underline{m} - \frac{1}{2s} \underline{x} \cdot \underline{x} - \frac{1}{2} \ln(1 - |\underline{m}|^2) \tag{A.10}$$

Using (A.1) this becomes

$$F(s, \underline{r}, \underline{x}) = 2\epsilon s + \underline{r} \cdot \underline{m} - \frac{1}{2} \ln(1 - |\underline{m}|^2) \tag{A.11}$$

Also notice that substituting (A.3) into (A.1) gives

$$\epsilon = -\frac{1}{2} \sum_{i=1}^{3} \lambda_i m_i^2 \tag{A.12}$$

This gives the closed form expression for the energy in terms of the magnetisation and coupling constants. Setting this into (A.11) and again using (A.3)

$$F(s, \underline{r}, \underline{x}) = -\sum_{i=1}^{3} m_i (x_i \sqrt{\lambda_i} - r_i) - \frac{1}{2} \ln(1 - |\underline{m}|^2) \tag{A.13}$$

Use (A.6) with (A.9) in F then this gives

$$\begin{aligned} F(s, \underline{r}, \underline{x}) &= -\frac{a}{\tanh a} |\underline{m}|^2 - \frac{1}{2} \ln(1 - |\underline{m}|^2) \\ &= -|\underline{m}| \tanh^{-1} |\underline{m}| - \frac{1}{2} \ln(1 - |\underline{m}|^2) \end{aligned} \tag{A.14}$$

APPENDIX B
Special cases of the coupling constants

Here we show the solutions to equations (9.12),(9.16) and (9.17) for the two special cases we considered in section 9.3 to express the entropy in terms of the total energy, u, and the external magnetic field, h.

B.1 The special case when $\lambda_1 = \lambda_2 = 0$, $\lambda_3 = 1$, $\underline{h} = |h|\cos\phi\hat{i} + |h|\sin\phi\hat{k}$

Using equation (9.12) we can find the expression for m_1,

$$m_1 = -\left(\frac{m_3^2 + 2hm_3\sin\phi + 2u}{2h\cos\phi}\right)^2 + m_3^2, \tag{B.1}$$

now substituting this into $|\underline{m}|$ and solving equations (9.16) and (9.17) gives

$$m_2 = 0 \tag{B.2}$$

$$\begin{aligned} m_3 \;=\; & -h\sin[\phi] + \frac{\left(-2u - 2h^4\cos[\phi]^4 + h^2\sin[\phi]^2\right)}{(3^{1/3} + 3^{-2/3})}\Big/ \\ & \left(9h^5\cos[\phi]^4\sin[\phi] \pm \frac{1}{3}\sqrt{729h^{10}\cos[\phi]^8\sin[\phi]^2 + \left(6u + 6h^4\cos[\phi]^4 - 3h^2\sin[\phi]^2\right)^3}\right)^{1/3} \end{aligned} \tag{B.3}$$

Note that the choice of the plus or minus sign depends on the sign of

$$\left(6u + 6h^4\cos[\phi]^4 - 3h^2\sin[\phi]^2\right)^3 \tag{B.4}$$

There are therefore two sets of solutions for (9.12), (9.16) and (9.17) corresponding to the ferromagnetic and paramagnetic phase. These solutions are not valid when $\phi = \pi/2$ since (B.3) then diverges. In this case the solution to $\underline{m}$ is only a single function that is equivalent to (9.22) for the isotropic Heisenberg model.

B.2 The special case when $\lambda_3 = 0$, λ_1, $\lambda_2 \in [0, 1]$ and $\underline{h} = |h|\,\hat{i}$

Here again we can find m_1 by using (9.12),

$$m_1 = -\frac{h}{\lambda_1} \pm \sqrt{\left(\frac{h}{\lambda_1}\right)^2 - \frac{\lambda_2 m_2^2}{\lambda_1} - \frac{2u}{\lambda_1}}, \tag{B.5}$$

now again if we solve (9.16) and (9.17) we get

$$\begin{aligned} m_2 &= \sqrt{-\frac{2u}{\lambda_2} + \frac{h^2(\lambda_1 - 4\lambda_2)}{2\lambda_2(\lambda_1 - 2\lambda_2)^2}}, \\ m_3 &= 0, \end{aligned} \tag{B.6}$$

or

$$\begin{aligned} m_2 &= 0, \\ m_3 &= 0, \end{aligned} \tag{B.7}$$

where equations (B.6) correspond to a maximum if $\lambda_2 > \lambda_1$ and equations (B.7) when $\lambda_2 < \lambda_1$. For equation (B.6) the plus or minus sign in m_1 depends on the sign of

$$-u + \frac{h^2(\lambda_1 - 4\lambda_2)}{2(\lambda_1 - 2\lambda_2)^2} \tag{B.8}$$

There are therefore two sets of solutions for equations (9.12), (9.16) and (9.17). These correspond to the ferromagnetic- and paramagnetic phases. When $\lambda_2 < \lambda_1$ the plus or minus sign in m_1 only depends on the sign of h so that only a ferromagnetic phase exists. The entropy here is equivalent to the isotropic Heisenberg model.

BIBLIOGRAPHY

[1] Casetti L and Nardini C, A solvable model of a self-gravitating system, 2010 J. Stat. Mech. P05006

[2] Levin Y, Pakter R and Teles TN, 2008 Phys. Rev. Lett. 100 40604

[3] Barre J, Dauxois T, De Ninno G, Fanelli D and Ruffo S, 2004 Phys. Rev. E 69 045501

[4] Dauxois T, Ruffo S and Cugliandolo F, 2008 Long-range interacting systems, Lecture notes of the Les Houches summer school: Volume 90.

[5] Pearce P A and Thompson C J, The anisotropic Heisenberg model in the long-range interaction limit , 1975 Commun. Math. Phys. 41 191

[6] Pflug A, Gravitating fermions in an infinite configuration space, 1980 Commun. Math. Phys. 78 83

[7] Campa A, Dauxois T and Ruffo S, Statistical mechanics and dynamics of solvable models with long-range interactions, 2009 Phys. Rep. 480 57

[8] Touchette H, When is a quantity extensive, and when is it additive?, Physica A 305. 2002.

[9] Truong L, Quantum microcanonical entropy of a pair of observables, 1974 Commun. Math. Phys. 39 207

[10] Bouchet F, Gupta S and Mukamel D, Thermodynamics and dynamics of systems with long-range interactions, 2010 Physica A 389 20, 4389-4405

[11] Eddington A.S, 1926 The internal constitution of the stars, Cambridge

[12] Thirring W, Systems with negative specific heat, 1970 Z. Phys. 235 339

[13] Lynden-Bell D and Wood R, The gravo-thermal catastrophe in isothermal spheres and the onset of red-giant structure for stellar systems, 1968 Mon. Not. R. Astron. Soc. 138 495

[14] Chavanis PH, 2006 Int. J. Mod. Phys. B20 3113

[15] Kinoshita T, Wenger T and Weiss DS, A quantum Newton's cradle, 2006 Nature. 440 900-903

[16] Ruelle D, Statistical mechanics: rigorous results, 1969 Benjamin, New York

[17] Baker GA, Ising model with a long-range interaction in the presence of residual short-range interactions, 1963 Phys. Rev. 130, 14061411

[18] Kac M, Uhlenbeck GE and Hemmer PC, On the van der Waals theory of the vapor-liquid equilibrium. I. Discussion of a one-dimensional model, 1963 J. Math. Phys. 4 216

[19] Touchette H, The large deviation approach to statistical mechanics, 2009 Phys. Rep. 478, 1-69

[20] Anteneodo C and Tsallis C, 1998 Phys. Rev. Lett. 80 5313

[21] Campa A, Ruffo S and Touchette H, Negative magnetic susceptibility and nonequivalent ensembles for the mean-field ϕ^4 spin model, 2007 Physica A 385, 233-248

[22] Touchette H, Ensemble equivalence for general many-body systems, 2011 arxiv:1106.2979

[23] Ellis RS, Haven K and Turkington B, 2000 J. Stat. Phys., 101 999.

[24] Dauxois T, Ruffo S, Arimondo E, Wilkens M, 2002 Dynamics and thermodynamics of systems with long-range interactions, Lecture notes in physics, vol. 602, Springer

[25] Gross DHE, Microcanonical thermodynamics, 2001 World Scientific, Singapore

[26] Kastner M, Nonequivalence of ensembles for long-range quantum spin systems in optical lattices, 2010 Phys. Rev. Lett. 104 240403

[27] Micheli A, Brennen GK and Zoller P, A toolbox for lattice-spin models with polar molecules, 2006 Nature Phys. 2 341

[28] ODell D, Giovanazzi S, Kurizki G and Akulin V M, BoseEinstein condensates with 1/r interatomic attraction: electromagnetically induced gravity, 2000 Phys. Rev. Lett. 84 5687

[29] Skvortsov AM, Klushin LI and Leermakers FA, Negative compressibility and nonequivalence of two statistical ensembles in the escape transition of a polymer chain, 2007 J. Chem. Phys. 126 024905

[30] Biskup M, Chayes L and Crawford N, Mean-field driven first-order phase transitions in systems with long-range interactions, 2006 J. Stat. Phys. 122 1139

[31] Chayes L, Mean-field analysis of low-dimensional systems, 2009 Commun. Math. Phys. 292 303

[32] Touchette H, Methods for calculating nonconcave entropies, 2010 J. Stat. Mech. P05008 (1-22)

[33] Arfken G, Mathematical methods for physicists, 1985 3rd ed. Orlando, FL: Academic Press, pp. 853-861

[34] Tindemans PAJ and Capel HW, An exact calculation of the free energy in systems with separable interactions, 1974 Physica 72 433

[35] Trotter HF, On the product of semi-groups of operators, 1959 Proc. Am. Math. Soc. 10 545

[36] Hubbard J, Calculation of partition functions, 1959 Phys. Rev. Lett. 3 77

[37] Stratonovich RL, On a method of calculating quantum distribution functions, 1958 Sov. Phys.Dokl. 2 416

[38] Bender CM and Orszag SA, Advanced mathematical methods for scientists and engineers, 1978 McGraw-Hill, New York, Chap. 10.

[39] Behringer H, Critical properties of the spherical model in the microcanonical formalism, 2005 J. Stat. Mech. P06014

[40] Rogers LJ, An extension of a certain theorem in inequalities, 1888 Messenger of Mathematics, New Series XVII (10): 145150

[41] Falk H, Inequalities of J. W. Gibbs, 1970 Am. J. Phys. 38, 858

[42] Tindemans PAJ and Capel HW, An exact calculation of the free energy in systems with separable interactions II, 1974 Physica 75 407